

pubs.acs.org/joc Article

Electrostatically Enhanced 3- and 4-Pyridyl Borate Salt Nucleophiles and Bases

Stephen H. Dempsey, Alex Lovstedt, and Steven R. Kass*



Cite This: J. Org. Chem. 2023, 88, 10525-10538



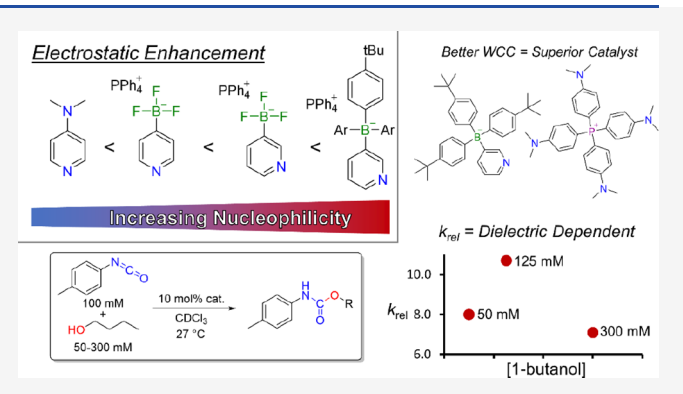
ACCESS I

III Metrics & More

Article Recommendations

Supporting Information

ABSTRACT: A variety of electrostatically enhanced 3- and 4-pyridylborate salt catalysts are reported and show significant improvement over an activated noncharged neutral control compound. Their nucleophilicity in a stoichiometric $S_{\rm N}2$ reaction and catalytic performance in a urethane synthesis are evaluated along with three methods for rapidly evaluating the basicity of these species. That is, qualitative titrations in ${\rm CH_2Cl_2}$ and ${\rm CHCl_3}$ were carried out, two separate solution-state IR studies in ${\rm CCl_4}$ and ${\rm CDCl_3}$ are reported, and the proton affinities of the anionic components of the salts were computed. Charge differences between the anion and its protonated zwitterionic conjugate acid are evaluated along with the highest occupied molecular orbitals of the anions in relationship to some of the surprising reactivity findings that were observed in the two kinetic studies.



■ INTRODUCTION

Organocatalysis is often viewed as a more environmentally friendly method than transition metal catalysis for enhancing reaction rates of a large variety of synthetic transformations. 1,2 Numerous acid and base systems have been thoroughly studied, and the desire for more potent catalysts is everpresent. In the former case, incorporation of electron withdrawing groups typically increases catalytic activity. One of the most effective and broadly applied substituents is the 3,5-bis(trifluoromethyl)phenyl ring, which possesses two strong electron withdrawing groups that stabilize the acid's conjugate base and enhance its catalytic activity.^{3,4} In our own work, we discovered that even larger rate enhancements can be obtained by employing positively charged substituents in combination with weakly coordinating anions. 5,6 For example, the incorporation of a cationic center as in 1-(N-methyl-3pyridinium)-3-phenylthiourea (Figure 1, left) when paired with tetrakis [3,5-bis(trifluoromethyl)phenyl]borate (BAr^F₄) was found to lead to an order of magnitude rate acceleration relative to bis(3,5-trifluoromethyl)phenylthiourea (Schreiner's thiourea, middle)³ in the Friedel-Crafts alkylation of Nmethylindole with *trans-\beta*-nitrostyrene.⁷ The addition of a second charged center in 1,3-bis(N-methyl-3-pyridinium)thiourea (right) led to a rate enhancement of an additional factor of 50. Similar effects were also found for 1,1'-bi-2naphthol (BINOL)-phosphoric acids^{8–10} and $\alpha,\alpha,\alpha',\alpha'$ -tetraaryl-2,2-disubstituted 1,3-dioxolane-4,5-dimethanol (TAD-DOLs),¹¹ and in conjunction with other groups,¹²⁻¹⁴ the broad applicability of this methodology has been demonstrated.

Small organic bases and nucleophiles are also of great interest. In the former case, a few motifs including guanidines, amidines, pyridines, and imidazoles have received the most attention. $^{15-24}$ From the very beginning of our efforts on charge-enhanced acids, we also envisioned using a negatively charged site to enhance basicity and nucleophilicity. Pyridine bases were initially targeted because they are commonly used proton acceptors, electron donating substituents are known to enhance their nucleophilicity and basicity, 25-27 and incorporation of a charged-center was expected to be synthetically straightforward making these compounds readily accessible. In this report, our initial efforts to generate charge-enhanced bases and nucleophiles using a series of 3- and 4-pyridylborates paired with different countercations are described (Figure 2). Their reactivities are compared not to pyridine but to 4dimethylaminopyridine (DMAP), a more reactive resonanceactivated analog in which the lone pair of electrons on the dimethylamino nitrogen atom is delocalized onto the pyridine ring nitrogen. More reactive DMAP derivatives are known (e.g., 4-(pyrrolidinyl)pyridine and 9-azajulolidine), 26-28 and Zipse's sulfonamide anion 4⁻PPh₄⁺ is currently the most active one,²⁸ so it is also contrasted to the pyridylborate anion salts

Received: March 8, 2023 Published: July 18, 2023





catalysts:
$$CF_3 \qquad CF_3 \qquad CF_$$

Figure 1. Thiourea-catalyzed Friedel-Crafts alkylation demonstrating the impact of charged substituents on reaction rates.

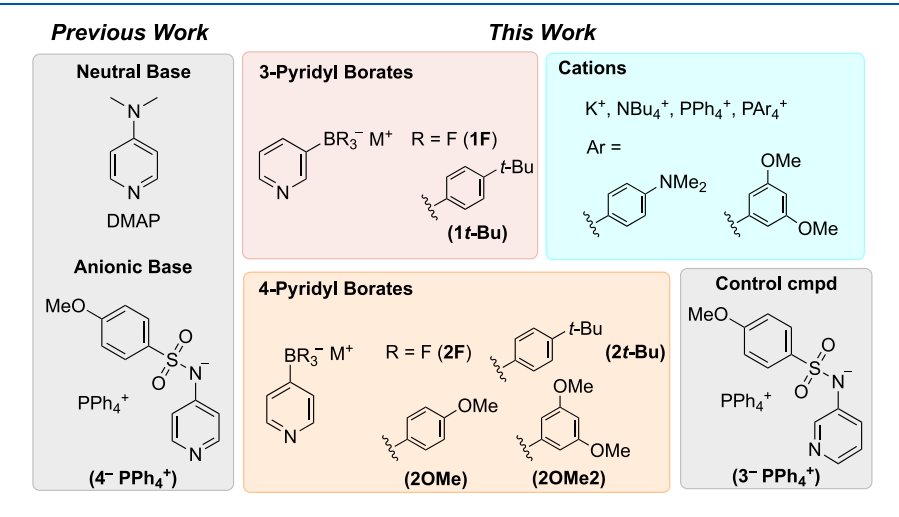


Figure 2. Borate salts and reference compounds examined in this study.

even though it can be viewed as an amide anion since the negative charge is partially delocalized onto the ring N-atom via resonance.

■ RESULTS AND DISCUSSION

Synthesis. Potassium salts of 3-pyridyltrifluoroborate ($1F^-K^+$) and 4-pyridyltrifluoroborate ($2F^-K^+$) have been previously synthesized and can be prepared on a multigram scale. They also provide ready access to their corresponding triarylborates by reacting them with aryl Grignard reagents (Scheme 1). Intriguingly, upon addition of $2F^-K^+$ (but not $1F^-K^+$) to the Grignard reagent and heating to reflux the solution turned deep blue, this color faded throughout the course of the reaction, and in each case, a white or off-white

Scheme 1. Synthetic Route for the Preparation of Triarylborate Salts Starting from Commercially Available Boronic Acids

HO BOH
$$BF_3$$
 K BF_3 K $BF_$

 $Ar = 4-t-BuC_6H_4$ (2t-Bu), $4-MeOC_6H_4$ (2OMe), $3.5-(MeO)_2C_6H_3$ (2OMe2)

solid product was formed. Three aryl derivatives of $2F^-$ K⁺ were synthesized (Ar = 4-t-BuC₆H₄ (2t-Bu⁻ K⁺), 4-MeOC₆H₄ ($2OMe^-$ K⁺), and 3,5-(MeO)₂C₆H₃ ($2OMe2^-$ K⁺)), but complex mixtures were obtained for the more electron-rich arene derivatives of $1F^-$ K⁺ (i.e., $1OMe^-$ K⁺ and $1OMe2^-$ K⁺). For both the 3- and 4-pyridyl derivatives, insoluble products were obtained in attempts to prepare Ar = 4-Me₂NC₆H₄. Switching the dimethylamino group to a dibutylamino substituent for improved solubility led to no greater success. A benchtop stable crystalline solid corresponding to a cyclic tetramer, however, was isolated in low yield from potassium 3-pyridyltrifluoroborate (eq 1).

$$\begin{array}{c} \text{BF}_3 \text{ K}^{\dagger} \\ \text{N} \\ \text{N} \\ \text{Ar} = 4\text{-Bu}_2 \text{NC}_6 \text{H}_4 \text{MgBr} \\ \text{Ar} \\ \text{$$

Conversions of the potassium salts of 1F⁻, 1*t*-Bu⁻, 2F⁻, 2*t*-Bu⁻, 2OMe⁻, and 2OMe2⁻ to their tetrabutylammonium (Bu₄N⁺) and tetraarylphosphonium (Ar₄P⁺) derivatives³¹ were accomplished via ion metathesis. For the latter species, the solubilities of KCl and KBr in water but not CH₂Cl₂ were exploited using biphasic conditions to afford the products in near-quantitative yields. The resulting salts were dried under

vacuum (<0.4 torr) and stored in a glovebox to exclude water. They are bench stable compounds over long periods of time (i.e., ≥ 6 months) and suitable crystals for X-ray crystallography were obtained for $1t\text{-Bu}^-\text{PPh}_4^+$ and $2t\text{-Bu}^-\text{PPh}_4^+$ (Figure 3) via benzene/pentane vapor diffusion.

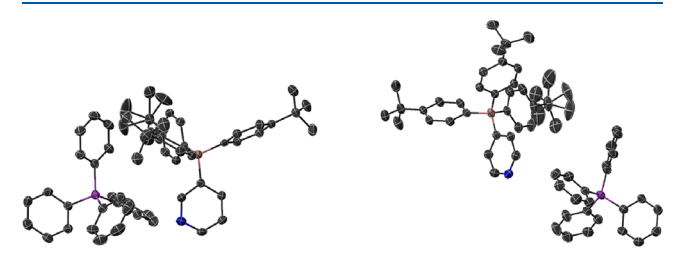


Figure 3. X-Ray crystal structures of 1*t*-Bu⁻PPh₄⁺ (left) and 2*t*-Bu⁻PPh₄⁺ (right) where the cocrystallized benzene and all of the hydrogen atoms are omitted for clarity. Atoms are drawn as thermal ellipsoids at the 50% probability level, with carbon, nitrogen, boron, and phosphorus atoms drawn as black, blue, pink, and purple respectively. See the Supporting Information for additional details.

 S_N2 Kinetics. Reactions of the substituted pyridine salts with 1-iodooctane were studied in dichloromethane under pseudo-first-order conditions at 25 °C (eq 2). Both UV-vis

and NMR spectroscopies were used to monitor reaction progress, and averaged results are given in Table 1 since there

Table 1. Reaction and Relative Rates for the S_N2 Reaction of Various Substituted Pyridines with 1-Iodooctane under Pseudo-First-Order Conditions at 25 $^{\circ}$ C

nucleophile	$k (\min^{-1})$	$k_{ m rel}$
DMAP ^a	0.00149	1.0
2F ⁻ PPh ₄ ⁺	0.00220	1.5
1F ⁻ PPh ₄ ⁺	0.00327	2.2
2OMe ⁻ PPh ₄ ⁺	0.00670	4.5
2t-Bu ⁻ PPh ₄ ⁺	0.00853	5.7
2OMe2 ⁻ PPh ₄ ⁺	0.00935	6.3
1t-Bu ⁻ P(3,5-(MeO) ₂ C ₆ H ₃) ₄ ⁺	0.0101	6.8
$4^- PPh_4^{+b}$	0.0110	7.4
1t-Bu PPh ₄ +	0.0148	9.9
1t-Bu ⁻ P(4-Me ₂ NC ₆ H ₄) ₄ ⁺	0.0159	10.7

 a DMAP = 4-dimethylaminopyridine. b Zipse's anionic DMAP analog illustrated in Figure 1.

is good accord between the two methods. The one exception is for $2F^-PPh_4^+$ where there was poor agreement between the two spectroscopic methods. In this case, only the NMR data were used because non-Beer's law behavior was observed in this instance.

Urethane Kinetics. Our charge-containing pyridylborates can serve not only as stoichiometric nucleophiles but also as catalytic bases. To explore this avenue of their reactivity, urethane formation was chosen (eq 3) in part because this functional group is used in many industrial products including insecticides, herbicides, and pharmaceutical chemicals. ³² Zipse et al. also has explored this process with a sulfonamide anion

where the pyridine ring nitrogen bears a negative charge (i.e., $4^-PPh_4^+$), and so, this compound makes for an interesting comparison along with its meta isomer ($3^-PPh_4^+$).

Reactions of 4-methylphenylisocyanate (100 mM) and 1-butanol (300 mM) with a 10 mol % catalyst loading were examined at 27 °C. Product conversions were monitored by ¹H NMR using the methylene resonances of the starting alcohol and resulting urethane, and linear fits of the data (see the Supporting Information) afforded the second-order rate constants (Table 2).

Table 2. Second-Order Rate Constants and Relative Rates for Urethane Formation

catalyst	$k \left(\mathrm{M}^{-1} \mathrm{min}^{-1} \right)$	$k_{ m rel}$
none	0.00512	0.071
4-MeOC ₆ H ₄ SO ₂ N ⁻ Ph PPh ₄ ⁺	0.0304	0.42
1F K+ + [2.2.2]cryptand	0.0554	0.77
2F ⁻ PPh ₄ ⁺	0.0630	0.87
DMAP	0.0722	1.0
$1F^- NBu_4^+$	0.0767	1.1
$1F^{-} P(3,5-(MeO)_{2}C_{6}H_{3})_{4}^{+}$	0.0772	1.1
3- PPh ₄ +	0.0976	1.4
1F ⁻ PPh ₄ ⁺	0.0994	1.4
$1F^{-}P(4-Me_{2}NC_{6}H_{4})_{4}^{+}$	0.118	1.6
2OMe ⁻ PPh ₄ ⁺	0.229	3.2
1t-Bu ⁻ PPh ₄ ⁺	0.263	3.6
2OMe2 ⁻ PPh ₄ ⁺	0.323	4.5
$2OMe2^{-} P(4-Me_2NC_6H_4)_4^{+}$	0.338	4.7
2t-Bu ⁻ PPh ₄ ⁺	0.375	5.2
1t-Bu ⁻ P(3,5-(MeO) ₂ C ₆ H ₃) ₄ ⁺	0.385	5.3
2t-Bu ⁻ P(4-Me ₂ NC ₆ H ₄) ₄ ⁺	0.410	5.7
1t-Bu ⁻ P(4-Me ₂ NC ₆ H ₄) ₄ ⁺	0.500	6.9
$4^- PPh_4^+$	0.517	7.2

Role of 1-Butanol. Charge-activated acids are less effective in polar solvents due to a diminishment of electrostatic effects. This also should be the case for charge-activated bases and nucleophiles, and while the urethane reaction is run in chloroform, which is a very low-polarity solvent ($\varepsilon = 4.72^{33}$), the inclusion of 1-butanol ($\varepsilon = 17.1^{33}$) increases the overall dielectric constant of the reaction medium. 1-Butanol is a hydrogen bond (H-Bond) donor as well, so its impact at two additional concentrations was examined (Table 3). All three rate constants using DMAP as the catalyst appear to be the same regardless of the 1-butanol concentration, whereas they vary with pyridine-containing salts. Variable time normalization kinetic analyses³⁴ of these data were consequently carried out to confirm the first-order dependence of 1-butanol. Plots of the product concentration versus $\Sigma[1\text{-butanol}]^{\alpha} \cdot \Delta t$ for $\alpha = 0$, 1, and 2 are consistent with a first-order dependence in each case (Figure 4 and the Supporting Information), although the fits are poor at the 50 mM concentration in some

 pK_a Determinations. Dilute solutions of DMAP and 1t-Bu⁻P(4-Me₂NC₆H₄)₄⁺ in chloroform and dichloromethane (~5 mM) were added to 9-cyanofluorene ($pK_a = 8.3$ in DMSO) and 9-carbomethoxyfluorene ($pK_a = 10.3$ in DMSO).³⁵ These indicators have colored conjugate bases,

Table 3. Second-Order Rate Constants and Relative Rates for Urethane Formation at Several 1-Butanol Concentrations

	[BuOH] = 300	mM	[BuOH] = 125	mM	[BuOH] = 50	mM
catalyst	$k \left(\mathbf{M}^{-1} \mathbf{min}^{-1} \right)$	$k_{\mathrm{rel}}^{}b}$	$k \left(\mathbf{M}^{-1} \ \mathbf{min}^{-1} \right)$	$k_{ m rel}$	$k \left(\mathbf{M}^{-1} \ \mathbf{min}^{-1} \right)$	$k_{ m rel}$
DMAP	0.0722	1.0	0.0651		0.0734	
$2F^-PPh_4^+$	0.0630	0.90	0.101	1.4	0.0978	1.4
1F ⁻ PPh ₄ ⁺	0.0994	1.4	0.134	1.9	0.111	1.6
2OMe ⁻ Ph ₄ P ⁺	0.229	3.3	0.412	5.9	0.294	4.2
$1t$ -Bu $^-$ Ph $_4$ P $^+$	0.263	3.7	0.393	5.6	0.431	6.1
$2OMe2^{-}Ph_{4}P^{+}$	0.323	4.6	0.557	7.9	0.336	4.8
$2t$ -Bu $^-$ Ph $_4$ P $^+$	0.375	5.3	0.638	9.1	0.375	5.3
1t-Bu ⁻ P(3,5-(MeO) ₂ C ₆ H ₃) ₄ ⁺	0.385	5.5	0.628	8.9	0.516	7.3
1t-Bu ⁻ P(4-Me ₂ NC ₆ H ₄) ₄ ⁺	0.500	7.1	0.739	10.5	0.565	8.0
$4^- Ph_4P^+$	0.517	7.4	0.727	10.4	0.610	8.7

^aReactions were run in CDCl₃ at 27 °C with 100 mM of 4-methylphenylisocyanate, 10 mM catalyst, and the indicated concentration of 1-butanol. ^bRelative rates are given in relation to the average of the DMAP rate constants for the three concentrations that were used.

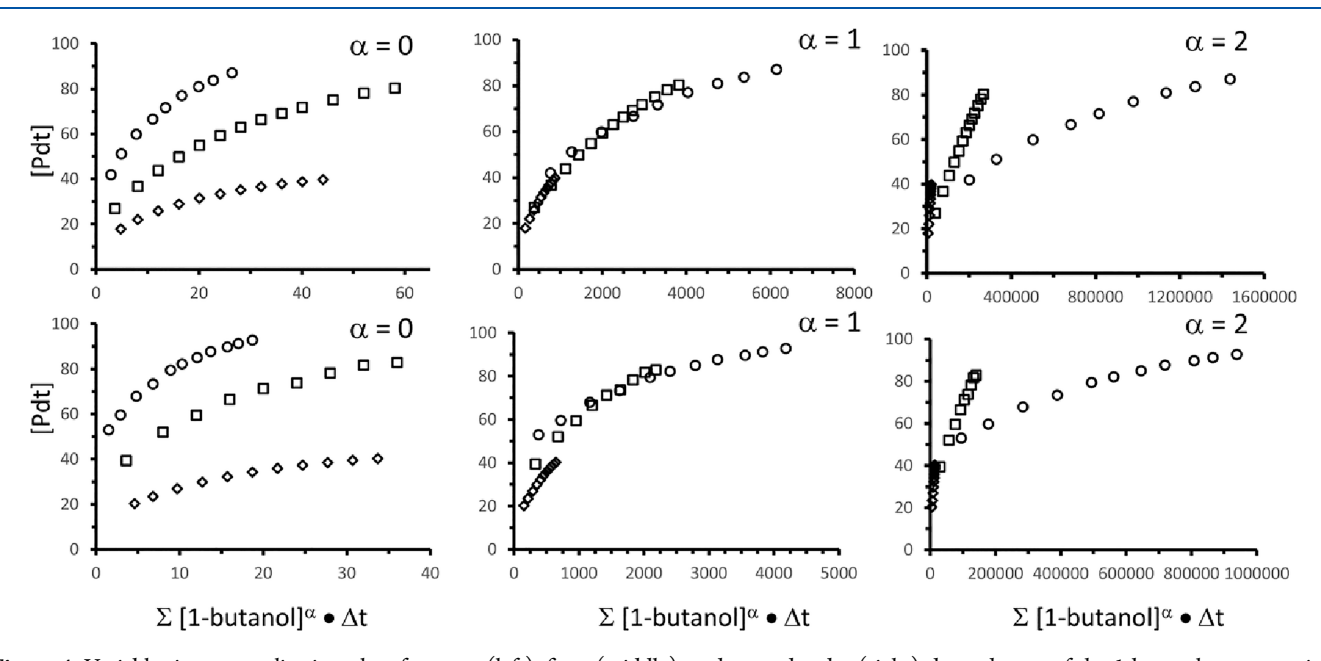


Figure 4. Variable time normalization plots for zero- (left), first- (middle), and second-order (right) dependences of the 1-butanol concentration using 1t-Bu $^-$ PPh $_4^+$ (top row) and 1t-Bu $^-$ P(4-Me $_2$ NC $_6$ H $_4$) $_4^+$ as the catalyst. Open circles, squares and diamonds are for [1-butanol] = 300, 125, and 50 mM, respectively, along with [4-methylphenylisocyanate] = 100 mM and [catalyst] = 10 mM.

and in both cases, a color change was observed with 9-cyanofluorene (i.e., the solution turned yellow) but not 9-carbomethoxyfluorene. This indicates that the conjugate acids of DMAP and 1t-Bu $^-$ P(4-Me $_2$ NC $_6$ H $_4$) $_4$ $^+$ have similar p K_a 's in chloroform and dichloromethane.

A second approach for assessing relative pK_a 's based upon liquid-phase IR spectroscopy was used. Jalue solutions of cyclohexanol in CCl_4 (1% v/v) in the presence and absence of a pyridine base (varying concentration, see the Supporting Information) were examined. A sharp O–H stretch was observed at 3622 cm⁻¹ in the latter case, and this band broadened and underwent a red shift of 210–330 cm⁻¹ upon the addition of various pyridine bases (Table 4). The resulting frequency shifts ($\Delta \nu$) linearly correlate with the previously measured gas-phase basicities of the pyridine derivatives (Figure 5); $\Delta \nu$ (cm⁻¹) = 4.68 ΔG° (kcal mol⁻¹) – 756, r^2 = 0.990. The measured frequency shift for 1t-Bu⁻P(4-Me₂NC₆H₄)₄+ (265 cm⁻¹), however, indicates that it is less basic than DMAP and similar to pyridine.

Infrared experiments were also carried out in CDCl₃, a solvent where the borate salts are significantly more soluble. In

Table 4. Infrared O-H Stretching Frequencies of Cyclohexanol in CCl₄ in the Presence of Different Pyridines along with Their Gas-Phase Basicities

cmpd	O-H (cm ⁻¹)	$\frac{\Delta \nu}{(\mathrm{cm}^{-1})}$	$\Delta G^{\circ a}$ (kcal mol ⁻¹)
DMAP	3293	329	232.1
4-trifluoromethylpyridine	3416	206	206.0
4 -pyridinecarboxaldehyde b	3401	221	208.6
3-bromopyridine	3400	222	209.9
3-acetylpyridine ^b	3382	240	211.4
pyridine	3371	251	214.7
1t-Bu ⁻ P(4-Me ₂ NC ₆ H ₄) ₄ ⁺	3357	265	

"Literature gas-phase basicity values taken from ref 36. ^bThe spectrum of the pyridine base in the absence of cyclohexanol was subtracted from that with the alcohol to obtain a corrected spectrum without the C=O stretch overtone, which overlaps with the shifted O-H band of interest.

this case the C–D stretching frequency was monitored in the presence and absence of different pyridine bases (Table 5).³¹

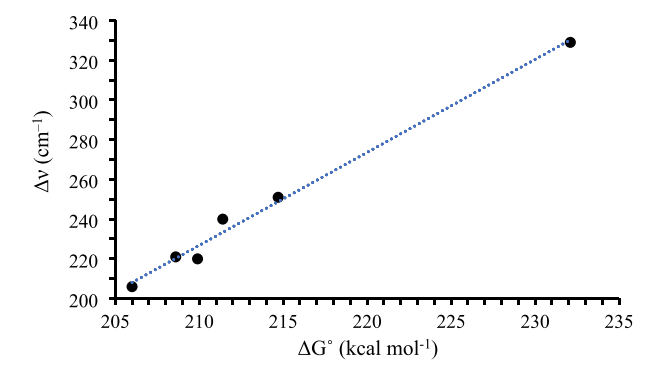


Figure 5. Linear least squares plot of IR O-H frequency shifts of cyclohexanol in the presence of pyridine bases $(\Delta \nu)$ vs the gas-phase basicities of the pyridine derivatives.

The resulting shifts are in the following order: pyridine < DMAP < salts, but this approach does not differentiate between the pyridines with charged substituents.

Table 5. Infrared C-D Stretching Frequencies of CDCl₃ in the Presence of Various Pyridine Derivatives^a

cmpd	$C-D (cm^{-1})$	$\Delta u \ ({ m cm}^{-1})$
pyridine	2224	29
DMAP	2210	43
$1F^-PPh_4^+$	2205	48
$2F^{-}PPh_{4}^{+}$	2203	50
$4^- PPh_4^+$	2203	50
1F [−] NBu ₄ ⁺	2202	51

^aThe D-CCl₃ stretch was observed at 2253 cm⁻¹ in the absence of pyridine bases.

Computations. Gas-phase proton affinities (PAs) were computed due to the relative ease of carrying out such calculations and our previous report, which found a good correlation between PAs and measured rate constants in nonpolar solvents (Table 6).5 These quantities were obtained by carrying out M06-2X geometry optimizations on both the bases and their conjugate acids with the aug-cc-pVDZ or ccpVDZ basis sets. For the conjugate acids and larger borates, the latter basis set was used, and aug-cc-pVDZ single-point energy determinations were subsequently carried out. This approach was tested with 1F and 2F by computing both

Table 6. Calculated PA of the Anions in This Study as well as Their Triphenylborate Derivatives

compound	PA (kcal mol ⁻¹)
DMAP	238.5 (238.4) ^a
1F ⁻	304.7
2F ⁻	302.4
1Ph ⁻	303.5
2Ph ⁻	301.9 ^b
1 <i>t</i> -Bu ⁻	303.2 ^b
$2t ext{-Bu}^-$	301.5 ^b
1OMe2	301.4 ^b
2OMe ⁻	302.9 ^b
2OMe2	297.9 ^b
4-	317.6
3-	307.2

^aExperimental value from ref 36. ^bSingle-point energies were used.

their M06-2X/aug-cc-pVDZ and M06-2X/aug-cc-pVDZ// M06-2X/cc-pVDZ proton affinities, and they differ by less than $0.1 \text{ kcal mol}^{-1}$.

pubs.acs.org/joc

As expected, all of the negatively charged pyridine derivatives are computed to be much more basic than DMAP. The PAs for 1F⁻, 2F⁻, 1t-Bu⁻, and 2t-Bu⁻ are all quite similar and only span a 3.2 kcal mol⁻¹ range. Sulfonamide anions 3 and 4, like the borate ions, are preferentially protonated at the ring nitrogen, but their PAs differ by 10.4 kcal mol⁻¹. This larger difference is not accounted for by the charge delocalization on to the pyridine nitrogen atom in 4since it is more basic than 3⁻ despite being 2.4 kcal mol⁻¹ more stable. This seeming contradiction is due to the 12.8 kcal mol⁻¹ greater stability of the conjugate acid resulting from 4⁻ and can be attributed to charge annihilation upon its protonation as opposed to zwitterion formation from 3⁻.

Counterion and solvation effects are not accounted for in these PA calculations, but all of the anions are found to be more basic than DMAP, and the following order is observed for the isomeric pairs of anions: $1F^- > 2F^-$, $1t-Bu^- > 2t-Bu^-$, and $4^- > 3^-$. These trends correlate with the S_N^2 reaction rates of these pyridines with 1-iodooctane in that the more basic anion reacts faster, and all of these nucleophiles outperform DMAP. For the urethane reaction, these trends break down and 2t-Bu > 1t-Bu and DMAP outperforms 1F K + [2.2.2] cryptand and 2F-PPh₄⁺.

Atomic polar tensor (APT) charges³⁷ were computed for 1F⁻, 2F⁻, 1t-Bu⁻, 2t-Bu⁻, 3⁻, and 4⁻and their conjugate acids, where the hydrogen contributions are summed into the atoms they are attached to (Table S35). The highest occupied molecular orbital (HOMO) and HOMO - 1 energies for all six anions were also examined and tabulated (Table 7).

Table 7. Computed M06-2X/aug-cc-pVDZ Frontier Molecular Orbital Energies

anion	HOMO (eV)	HOMO - 1 (eV)
1F ⁻	$-4.63 \ (\pi)$	$-4.84~(\sigma)$
2F-	$-4.87 (\pi)$	$-4.89 (\sigma)$
1 <i>t</i> -Bu ⁻	$-4.29 (\sigma)$	$-4.38 \; (\pi)$
$2t$ -Bu $^-$	$-4.32~(\sigma)$	$-4.48 \; (\pi)$
3-	$-3.09 (\pi)$	$-4.72~(\sigma)$
4-	$-3.33 (\pi)$	$-4.94 (\pi), -5.09 (\sigma)^a$
a HOMO – 2.		

The nucleophilicity ranking determined by the alkylation kinetics demonstrates the promise of the charge-incorporation strategy. All of the negatively charged pyridine derivatives that we examined are more nucleophilic than DMAP, and the most potent compound, 1t-Bu P(4-Me₂NC₆H₄)₄ reacts an order of magnitude more rapidly. It is also faster than Zipse's anionic DMAP analog, 4⁻ PPh₄^{+,28} even though this latter species is a vinylogous amide with a resonance delocalized negative charge on the pyridine ring nitrogen atom. There are no analogous resonance structures for the pyridylborates, but we initially expected the 4-pyridylborates to be more electron-rich and nucleophilic at the nitrogen center than the corresponding 3pyridylborates. This was based upon polarization of the C-B bond, delocalization of the resulting negative charge onto the nitrogen atom, and the greater stability of the 4- vs 3-pyridyl anion in the gas phase.

In accord with this view, the computed APT charges are more negative on the nitrogen atoms of the 4-pyridyl derivatives (i.e., $-0.48 (2F^{-}) \text{ vs } -0.42 (1F^{-}), -0.52 (2t-Bu^{-})$ vs -0.41 (1*t*-Bu⁻), and -0.72 (4⁻) vs -0.26 (3⁻)). However, in the two direct available comparisons between the 3- and 4pyridylborates, the former species react faster! That is, the alkylation rate constant for 1F-PPh₄⁺ is 1.5× larger than for $2F^{-}PPh_4^{+}$ and it is 1.7× bigger for 1t-Bu $^{-}PPh_4^{+}$ than 2t-Bu⁻PPh₄⁺. These results are in agreement with the computed gas-phase proton affinities, which indicate that the 3-pyridyl derivatives are more basic than their 4-pyridyl isomers (i.e., PA $(1F^{-}PPh_{4}^{+} - 2F^{-}PPh_{4}^{+}) = 2.3 \text{ kcal mol}^{-1} \text{ and PA } (1t-Bu^{-}PPh_{4}^{+} - 2t-Bu^{-}PPh_{4}^{+}) = 1.7 \text{ kcal mol}^{-1}).$ They also correlate with changes in the charges as modeled by the borate anions and their conjugate acids. That is, the charge at the nitrogen atom in the conjugate acid minus the corresponding value in the anion is larger for the 3-pyridyl derivatives than their 4-pyridyl isomers (Table S35). This suggests that the 4pyridylborate anions are more stable than the 3-pyridylborate ions because of their greater charge delocalization. In contrast, the zwitterionic products formed upon alkylation of the 3pyridylborates are more stable than those arising from the 4pyridylborates due to the shorter distance between the oppositely charged centers. Our computations are in accord with this explanation, in that 2F and 2t-Bu are 1.3 and 1.6 kcal mol⁻¹ more stable than 1F⁻ and 1t-Bu⁻, respectively, and protonated 1F and 1t-Bu are 1.0 and 0.1 kcal mol⁻¹ more stable than the conjugate acids of 2F and 2t-Bu. A plot of the logarithm of the pseudo-first-order S_N2 rate constants versus the HOMO or HOMO - 1 energy involving the nitrogen lone pair of electrons in the borate salts is linearly correlated (Figure 6). Frontier molecular orbital theory thus accounts for their relative reactivity, but not the structurally distinct sulfonamide anions.

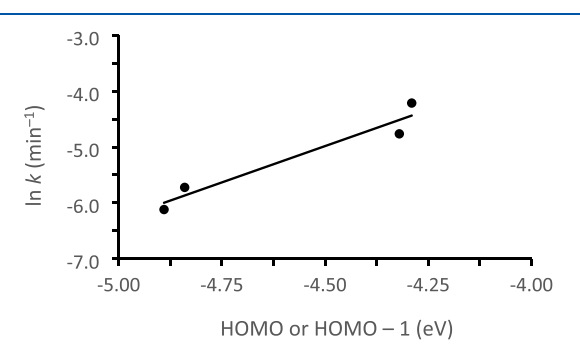


Figure 6. Plot of $\ln k \, (\text{min}^{-1})$ for the $S_N 2$ reaction of 1-iodooctane and tetraphenylphosphonium ion borate salts versus the latter anions M06-2X/aug-cc-pVDZ HOMO or HOMO -1 energies in eV; $\ln k = 2.60 \times \text{HOMO}$ (or HOMO -1) + 6.72, $r^2 = 0.935$.

Substitution of the fluorines in the pyridyltrifluoroborates $1F^-$ and $2F^-$ with a less electron withdrawing group (i.e., $\sigma_{\rm meta} = 0.05$ (Ph) vs 0.34 (F))³⁹ was expected to enhance the nucleophilicity and both $1t\text{-Bu}^-$ and $2t\text{-Bu}^-$ are more reactive than $1F^-$ and $2F^-$. Incorporation of a stronger electron donating group than t-Bu on to the aromatic ring as in $2OMe^ PPh_4^+$ and $2OMe2^ PPh_4^+$ led to slight diminishment and enhancement in the reactivity, respectively with rate constants in the following order: $k_{2OMe^-PPh4^+} < k_{2t\text{-Bu}^-PPh4^+} < k_{2t\text{-Bu}^-PPh4^+} < k_{2OMe^-PPh4^+}$. Intriguingly, this reactivity order and that of $1t\text{-Bu}^-$ vs $1F^-$ and $2t\text{-Bu}^-$ vs $2F^-$ are inversely related to the proton affinities of the anions (i.e., PA $(2OMe^-)$ < PA $(2t\text{-Bu}^-)$ < PA $(2OMe2^-)$, PA $(1t\text{-Bu}^-)$ < PA $(1t\text{-Bu}^-)$ < PA $(2t\text{-Bu}^-)$ < PA $(2t\text{-Bu}^-)$

and/or solvation effects play a critical role in these reactions. $^{40-46}$

In a previous study, tetraphenylphosphonium ions bearing electron donating substituents such as $P(4-Me_2NC_6H_4)_4^+$ and $P(3.5-(MeO)_2C_6H_3)_4^+$ were found to enhance the S_N2 reactivity of Cl with 1-iodooctane by factors of 6 and 7 relative to PPh₄⁺ Cl⁻³¹ Similar rate enhancements for 1t-Bu-PPh₄+ might be expected too, but the impact of these two cations is quite modest in this case (i.e., $k_{rel} = 1.00 \text{ (PPh}_4^+)$, 1.07 (P(4-Me₂NC₆H₄)₄⁺), and 0.68 (P(3,5-(MeO)₂C₆H₃)₄⁺)). This could be explained if 1t-Bu-PPh₄+ exists predominantly as free ions, but this is unlikely since CH2Cl2 is a nonpolar solvent. The tetraphenylphosphonium ion can function as a weak multiple hydrogen bond donor by making use of several of its ortho-ring hydrogens, and the pyridine ring nitrogen is a strong hydrogen bond acceptor. Interactions of this sort between the cation and anion are of considerable interest as they can have a significant effect on the reactivity of salts and will be the subject of subsequent investigations.

Rapid IR assays for assessing the reactivities of pyridinebased nucleophiles and bases were sought for the identification of lead compounds. Two approaches based upon previous work from our group were explored.^{5,31} In the first, the hydrogen bound O-H stretches of cyclohexanol in the presence of a series of six neutral pyridines with known gasphase basicities (ΔG° for the reaction BH⁺ \rightarrow B + H⁺) were measured and compared to its free O-H absorption at 3622 cm⁻¹ in CCl₄ (i.e., $\Delta \nu$). An excellent linear correlation ($r^2 =$ 0.99) between $\Delta \nu$ and the experimental values for ΔG° was obtained. This presumably correlates with the relative reactivities of these pyridines with 1-iodooctane, but $\Delta \nu$ for 1t-Bu⁻P(4-Me₂NC₆H₄)₄⁺ is much lower than expected. It's predicted basicity and reactivity based upon this value are between that of pyridine and DMAP. This is in accord with the pK_a determination in CHCl₃ and CH₂Cl₂ but at odds with its reactivity. A compensation effect in which more than one molecule of cyclohexanol interacts with the basic site of the charged pyridine ring may account for this discrepancy and is in keeping with a similar explanation for the IR spectra of a series of weakly coordinating cations' chloride salts.3 Alternatively, rather than doping the solution with a hydrogen bond donor, a solvent with a weak hydrogen bond donating ability (i.e., CDCl₃) was used. This approach predicts that pyridine and DMAP are less basic and reactive than $1F^-NBu_4^+$, $1F^-PPh_4^+$, $2F^-PPh_4^+$, and $4^-PPh_4^+$ but the $\Delta\nu$ values for these salts only span a 3 cm⁻¹ range, which is too small to differentiate between these compounds. Further development will be needed to elucidate the role of the countercation and for this to become a generally useful method for the rapid evaluation of charge-enhanced nucleophiles and bases.

The pyridylborate salts reported in this work not only can function as stoichiometric nucleophiles, but they also can be used as bases in a catalytic fashion. This was explored in the urethane forming reaction of 4-methylphenylisocyanate with 1-butanol (eq 3). In an analogous fashion to the $S_{\rm N}2$ reaction, the most effective pyridylborate catalyst is $1t\text{-Bu}^-\text{P}(4\text{-Me}_2\text{NC}_6\text{H}_4)_4^+$ and the borate salts are better catalysts than DMAP with the exception of $1\text{F}^-\text{K}^+$ with added [2.2.2]-cryptand and $2\text{F}^-\text{PPh}_4^+$. In these cases, the counterions play a more significant role in determining the reaction rates. The reactivity order for the urethane reactions is different than the

Pathway B

Figure 7. Two different pathways for the urethane reaction catalyzed by 1t-Bu-PPh₄⁺.

 $S_{
m N}2$ transformations, but once again, the charged catalysts outperform DMAP by up to an order of magnitude.

Given the importance of the counterion in both the S_N2 and urethane-forming transformations with the pyridylborates, it is unlikely that free ions are the reactive species in these two processes. This is generally consistent with what is known about salts in nonpolar solvents 44,47 and suggests that ion pairs and/or aggregates play a key role in both reactions. To assess this further, different concentrations of 1-butanol were screened to evaluate its impact on the reaction medium. We anticipated increases in the relative rate constants of the pyridylborate salts compared to DMAP with a decrease in the 1-butanol concentration due to the greater electrostatic effects in the former species, and in accord with our initial report on charge-activated acids.⁵ Surprisingly, the catalyst activity was highest at the intermediate concentration studied (i.e., 125 vs 300 and 50 mM) for all but one of the charged species (i.e., 1t-Bu⁻Ph₄P⁺). Variable time normalization analyses of the data (see the Supporting Information) indicated first-order behavior with respect to 1-butanol, but there is some deviation in the 50 mM results for some of the salts. This suggests that the reactive species or possibly the mechanism changes at the lowest concentration of 1-butanol. Further studies are needed to determine the cause of this behavior, but a possibility is that the reaction pathway changes upon making 1-butanol the limiting reagent (i.e., [1-butanol] = 50 mM, [4-methylphenylisocyanate] = 100 mM, and [catalyst] = 10 mM, Figure 7). Nucleophilic catalysts are generally thought to react through pathway A, with addition to the isocyanate taking place first.^{27,48,49} Other amine bases, however, have been shown to proceed through pathway B.^{50,51} It is possible to imagine these catalysts proceeding via either route, and the amount of 1butanol in solution could impact which pathway dominates.

Three additional catalysts were examined in the urethane-forming reaction: Zipse's highly effective anionic DMAP analog $(4^-Ph_4P^+)^{28}$ it's 3-pyridyl isomer $(3^-Ph_4P^+)$, and a derivative where the pyridine ring is replaced by a phenyl group $(4\text{-MeOC}_6H_4\text{SO}_2\text{N}^-\text{Ph}\ Ph_4P^+)$. For this sulfonamide system, the positioning of the pyridine nitrogen relative to the anionic center is important. The 4-pyridyl anion is 5 times more active than its 3-isomer due to resonance delocalization of the charge on to the ring nitrogen in 4^- , something that does not take place in 3^- or any of our pyridylborates.

Substitution of the pyridine ring with a phenyl group in either isomer leads to the same compound (4-MeOC₆H₄SO₂N⁻Ph Ph₄P⁺), and while it is 3.5 times less effective than $3^-Ph_4P^+$ and 2.5 times poorer than DMAP, it still is able to catalyze urethane formation.

CONCLUSIONS

The nucleophilicity ranking determined by the alkylation kinetics demonstrates the promise of the charge-incorporation strategy. All of the negatively charged pyridine derivatives that were examined are more nucleophilic than DMAP, and the most potent compound 1t-Bu⁻P(4-Me₂NC₆H₄)₄ is more reactive by more than a factor of 10. In the urethane forming reaction, all of the charged pyridine-containing salts with two exceptions $(1F^-K^+ + [2.2.2] \text{ cryptand and } 2F^-PPh_4^+)$ are also better catalysts than DMAP. The most active derivative is again 1t-Bu⁻P(4-Me₂NC₆H₄)₄⁺, and it leads to a rate enhancement of up to a factor of 11. All of the borate salt catalysts with one exception (1t-Bu-Ph₄P+) achieve their highest reaction rate constants at the intermediate concentration of 1-butanol (i.e., 125 mM rather than 50 or 300 mM), surprisingly rather than in the reaction mixture with the lowest dielectric constant, that is, the one containing 50 mM 1-butanol. Variable time normalization analyses of the kinetic data indicate that there is some deviation from first-order behavior when 1-butanol becomes the limiting reagent, possibly because the reactive species changes with its concentration.

The 3-pyridyl borates are consistently more effective than their 4-pyridyl counterparts. This is consistent with their slightly greater computed proton affinities and a linear correlation between the highest occupied molecular orbitals and logarithm of the $\rm S_{\rm N}2$ pseudo-first-order rate constants. In solution, these salts may adopt a variety of possible forms (i.e., solvent separated and contact ion pairs, ion triplets, or larger aggregates, as well as free ions), and ongoing studies are being carried out to address these intricacies with the aim of applying the charge-enhancement methodology to more basic substrates such as amidines, guanidines, and chiral alkaloids for asymmetric catalysis. Incorporation of an asymmetric center at boron also can be envisioned and may facilitate enantioselective transformations in an analogous fashion to chiral functionalized DMAP derivatives. $^{\rm 52-56}$

pubs.acs.org/joc

EXPERIMENTAL SECTION

General. Aryl bromides and tetraphenylphosphonium chloride and bromide were purchased from Oakwood Chemical. 3- and 4-Pyridylboronic acids came from Ambeed, while HPLC-grade methanol, dichloromethane (DCM), tetrahydrofuran (THF), diethyl ether, and anhydrous K_2CO_3 were obtained from Fisher Scientific. Deuterated solvents were acquired from Cambridge Isotope Laboratories, and all other reagents and solvents were purchased from Sigma-Aldrich. Substituted tetraarylphosphonium chlorides were previously synthesized according to published procedures. 31

Glassware was dried in an oven at 120 °C and allowed to cool under a stream of argon. Alumina and molecular sieves were activated and stored in a kiln at 300 °C. Dry and degassed THF, DCM, and diethyl ether were taken from a commercial solvent drying system. Deuterated chloroform was treated with anhydrous K₂CO₃ and dried over 3 Å molecular sieves for 24 h prior to use. Deuterated DCM was dried with 3 Å molecular sieves for 24 h. Aryl bromides and 1-iodooctane were purified by passing them through activated alumina, stored under argon, and used within 48 h. 1-Butanol was dried by passing it through an activated alumina column and stored over 3 Å molecular sieves under argon. Carbon tetrachloride and cyclohexanol were dried over activated 3 Å sieves for 4 d under argon. All other reagents were used as purchased.

NMR spectra were recorded on 400 and 500 MHz spectrometers. Chemical shifts are given in ppm and were referenced as follows: δ 7.27 (CDCl₃, 1 H), δ 77.0 (CDCl₃, 13 C), δ 5.32 (CD₂Cl₂, 1 H), δ 54.00 (CD₂Cl₂, 13 C), δ 2.05 (acetone-d₆, 1 H), δ 29.84 (acetone-d₆, 13 C), δ 3.31 (methanol- d_4 , ¹H), δ 49.00 (methanol- d_4 , ¹³C) δ -78.5 (¹⁹F, CF₃CO₂H, external calibrant). ³¹P shifts were referenced through the deuterium lock channel according to the IUPAC unified scale.³⁷ ¹¹B spectra were taken with background suppression unless otherwise noted. Titrations of these compounds revealed distinct changes in peak shapes depending on concentration, which can completely obscure the relevant coupling. Situations where, for example, singlets are seen instead of doublets for pyridyl hydrogens are due to this phenomenon. Unexpected coupling patterns are also observed in some heteronuclear spectra. Data workup using MestReNova's peak deconvolution allowed access to coupling information for some spectra where shimming and splitting patterns were perturbed by high salt concentration, but not all datasets were amenable to this treatment. Some coupling partners are therefore absent, but all visible J-values (or those that could be accessed via deconvolution) are included. Additionally, some 13C resonances are weak enough (particularly the quaternary carbons adjacent to a boron center) so as not to be seen. Attempts to observe the signals through the proton channel via HMBC were unsuccessful, but the combination of ¹³C spectra and HRMS data provide definitive confirmation of the compounds' identity. Spectra with missing resonances are noted.

Uncorrected melting points were recorded using unsealed capillary tubes. High-resolution mass spectra were collected with an ESI-TOF instrument using solutions in acetonitrile. Polyethylene glycol (PEG) was used as an internal calibrant for positive spectra, and a proprietary standard solution from SciEx with four known components was used for negative spectra. Fourier transform IR spectra were recorded with a spectrometer equipped with a laminated diamond-attenuated total reflection (ATR) attachment for all solid samples and a transmission cell with NaCl windows and a 0.1 mm path length for the liquid phase studies. For solid samples, nondiagnostic IR bands above 3200 cm⁻¹ were excluded since many of the compounds are hygroscopic and the spectra were recorded out in the open. UV-vis kinetic data were collected using a spectrometer equipped with an 8 cell Peltier temperature controlled apparatus. Threaded 10 mm quartz cuvettes equipped with Mininert caps were used in all cases to ensure an inert and moisture free atmosphere over the course of the reactions. The cuvettes were sealed with electrical tape and Parafilm as an added

Potassium Trifluoro(pyridin-3-yl)borate (1F⁻ K⁺). This compound was synthesized according to a previous report with only minor alterations.²⁹ 3-Pyridylboronic acid (1.85 g, 15.1 mmol, 1.00 equiv)

was suspended in 10 mL of methanol in a 50 mL round-bottomed flask under an argon atmosphere and cooled with an ice water bath. KHF₂ (3.53 g, 45.2 mmol, 2.99 equiv) and water (12.0 mL, 0.67 mol, 44.4 equiv) were added in one part. The cooled mixture was stirred for 30 min before being allowed to warm to room temperature where it was maintained for 18 h. The solvent was then removed under reduced pressure, and the resulting crude white powder was boiled in 80 mL of acetone and subsequently filtered. The solid was returned to the 125 mL Erlenmeyer flask and the boiling and filtering process was repeated three times in total. Concentration of the combined acetone solutions to ~100 mL was followed by the addition of 3.00 g (21.7 mmol, 1.4 equiv) of K₂CO₃, and the resulting suspension was boiled overnight. Filtration of the hot mixture and concentration of the solution under reduced pressure led to a solid that was dissolved in a minimal amount of methanol, which was then triturated into 200 mL of ether. The resulting solid was isolated by filtration and dried under vacuum to afford 1.88 g (10.1 mmol, 65%) of the potassium salt with spectra that are in accord with the literature.²⁹ ¹H NMR (500 MHz, $(CD_3OD) \delta 8.58$ (s, 1H), 8.28 (dd, J = 5.0, 1.9 Hz, 1H), 7.92 (dt, J = 5.0) 7.5, 1.8 Hz, 1H), 7.24 (dd, J = 7.5, 5.0 Hz, 1H). ¹¹B NMR (128 MHz, CD₃OD) δ 3.32 (d, J = 51.8 Hz). ¹³C{H} NMR (126 MHz, CD₃OD) [missing one resonance] δ 152.4, 146.9, 141.8, 124.3. 19 F{H} NMR (471 MHz, CD₃OD) δ –144.21 (q $J_{\text{F-B}}$ = 72.1, 37.0 Hz).

Potassium Trifluoro(pyridin-4-yl)borate (2**F** K^+). 4-Pyridylboronic acid (2.15 g, 17.5 mmol, 1.00 equiv) and KHF₂ (4.09 g, 52.4 mmol, 2.99 equiv) afforded the crude trifluoroborate using the same procedure as for the trifluoro(pyridin-3-yl)borate. The crude solid material was taken up in minimal methanol (~80 mL) and triturated into 200 mL of ether to afford 1.58 g (8.50 mmol, 49%) of the potassium salt. This compound previously was commercially available. ⁵⁸ ¹H NMR (500 MHz, acetone- d_6) δ 8.26 (d, J = 5.5 Hz, 2H), 7.35 (d, J = 4.6 Hz, 2H). ¹¹B NMR (161 MHz, CD₃OD) δ 2.75 (d, J = 42.9 Hz). ¹³C{H} NMR (126 MHz, CD₃OD) [missing 1 resonance] δ 147.5, 128.7. ¹⁹F{H} NMR (471 MHz, acetone- d_6) δ –144.62 (q, J = 49.4 Hz).

Tetrabutylammonium Trifluoro(pyridin-3-yl)borate (1**F**- NBu₄+). In a 20 mL vial, potassium trifluoro(pyridin-3-yl)borate (231 mg, 1.25 mmol, 1.00 equiv) and tetrabutylammonium chloride (347 mg, 1.25 mmol, 1.00 equiv) were dissolved in ACN and stirred for 30 min. The resulting suspension was filtered through tightly packed Celite and concentrated under reduced pressure to afford 474.8 mg (1.22 mmol, 98%) of the tetrabutylammonium salt as a white powder (m.p. = 59-61 °C). Spectra are in agreement with literature values. 59,60 3069, 3014, 2963, 2878, 1580, 1565, 1493, 1396, 1211, 1000, 997, 949, 808, 727 cm⁻¹. 1 H NMR (500 MHz, CDCl₃) δ 8.71 (s, 1H), 8.34 (d, J = 4.9 Hz, 1H), 7.84 (d, J = 7.6 Hz, 1H), 7.09 (t, J = 6.2 Hz, 1H), 3.02 (t, J = 7.4 Hz, 8H), 1.47 (quintet, J = 7.6 Hz, 8H), 1.31(sextet, I = 7.4 Hz, 8H), 0.93 (t, I = 7.4 Hz, 12H). ¹¹B NMR (161 MHz, CDCl₃) δ 3.24. ¹³C{H} NMR (126 MHz, CDCl₃) δ 153.0, 146.8, 139.56, 122.6, 58.3, 23.7, 19.5, 13.5. ¹⁹F{H} NMR (471 MHz, CDCl₃) δ -141.67. HRMS-ESI calcd for C₁₆H₃₆N⁺ (M - 1F⁻)⁺ 242.2483, found 242.2486 and calcd for $C_5H_4BF_3N^ (M-NBu_4^+)^-$ 146.0394, found 146.0388.

Tetraphenylphosphonium Trifluoro(pyridin-3-yl)borate (1F-PPh₄⁺). Tetraphenylphosphonium chloride (600 mg, 1.60 mmol, 1.00 equiv) and potassium trifluoro(pyridin-3-yl)borate (608 mg, 1.62 mmol, 1.01 equiv) were dissolved in 5 mL of DCM and stirred vigorously with 5 mL of dilute K2CO3 in water for 1 h. Upon addition of 10 mL of DCM and separation of the organic layer, concentration under reduced pressure afforded 738 mg (1.52 mmol, 94%) of the tetraphenylphos-phonium salt as a white powder (m.p. = 174-177 °C). IR-ATR 3067, 3017, 2991, 1587, 1564, 1442, 1436, 1215, 1108, 986, 951, 757, 719, 686 cm⁻¹. ¹H NMR (500 MHz, CDCl₃) δ 8.68 (s, 1H), 8.25 (d, J = 5.0 Hz, 1H), 7.94 (d, J = 7.4 Hz, 1H), 7.86 (td, J =7.4, 2.0 Hz, 4H), 7.73 (td, J = 7.9, 3.5 Hz, 8H), 7.63–7.50 (m, 8H), 7.07 (dd, J = 7.4, 4.9 Hz, 1H). ¹¹B NMR (161 MHz, CDCl₃) δ 3.14 (d, $J_{B-F} = 52.0 \text{ Hz}$). ¹³C{H} NMR (126 MHz, CDCl₃) δ 152.8, 146.1, 140.2, 135.8 (d, J_{P-C} = 3.2 Hz), 134.4 (d, J_{P-C} = 10.3 Hz), 130.8 (d, J_{P-C} = 12.8 Hz), 122.5, 117.5 (d, J_{P-C} = 89.5 Hz). ¹⁹F{H} NMR (471 MHz, CDCl₃) δ –144.06. ³¹P{H} NMR (203 MHz, CDCl₃) δ 23.13.

HRMS-ESI calcd for $C_{24}H_{20}P^+$ (M - 1 F^-) $^+$ 339.1298 found 339.1304 and calcd for $C_5H_4BF_3N^-$ (M - PPh $_4^+$) $^-$ 146.0394, found 146.0399.

Tetrakis[4-(dimethylamino)phenyl]phosphonium Trifluoro-(pyridin-3-yl)borate ($1F^ P(4-Me_2NC_6H_4)_4^+$). Tetrakis(4-(dimethylamino)phenyl)phosphonium chloride (79.2 mg, 0.145 mmol, 1.05 equiv) and potassium trifluoro-3-pyridylborate (72.7 mg, 0.138 mmol, 1.00 equiv) afforded the product in 97% yield (88.1 mg, 0.133 mmol) as a pale yellow solid (m.p. = 161-163 °C) using the same procedure as the tetraphenylphosphonium salt 1F-PPh₄⁺. This compound appears to decompose slowly in solution based on the presence of a characteristic BF_4^- peak in the ^{19}F NMR. IR-ATR 3010, 2985, 1590, 1516, 1369, 1206, 1103, 991, 942, 817, 800, 773 cm⁻¹. ¹H NMR (500 MHz, acetone- d_6) δ 8.68 (s, 1H), 8.19 (s, 1H), 7.78-7.66 (m, 1H), 7.45-7.30 (m, 8H), 7.03-6.87 (m, 9H), 3.11 (s, 24H). 11 B NMR (128 MHz, acetone- d_6) δ 2.98 (q, $J_{\text{B-F}}$ = 51.0 Hz). 13 C{H} NMR (126 MHz, acetone- d_6) [missing 1 resonance] δ 154.6, 154.4, 146.8, 139.6, 135.9 (d, J_{P-C} = 11.6 Hz), 122.7, 113.0 (d, J_{P-C} = 13.2 Hz), 104.7 (d, J_{P-C} = 103.4 Hz), 40.0. ¹⁹F{H} NMR (471 MHz, acetone- d_6) δ -142.86 (dd, $J_{\text{F-B}}$ = 101.1, 50.2 Hz). ³¹P{H} NMR (203 MHz, CDCl₃) δ 18.76. HRMS-ESI calcd for $C_{32}H_{40}N_4P^+$ (M – $1F^{-}$)⁺ 511.2986 found 511.2982 and calcd for $C_5H_4BF_3N^{-}$ (M - $P(4-Me_2NC_6H_4)_4^+)^-$ 146.0394, found 146.0402.

Tetrakis(3,5-dimethoxyphenyl)phosphonium Trifluoro(pyridin-3yl)borate $(1F^- P(3,5-(MeO)_2C_6H_3)_4^+)$. Tetrakis (3,5dimethoxyphenyl)phosphonium chloride (82.7 mg, 0.135 mmol, 1.05 equiv) and potassium trifluoro-3-pyridylborate (67.6 mg, 0.128 mmol, 1.00 equiv) afforded 88.2 mg (0.122 mmol, 95%) of the product as a pale brownish-red solid (m.p. >220 °C) using the same procedure as the tetraphenylphosphonium salt 1F⁻PPh₄⁺. IR-ATR 3077, 3011, 2940, 2840, 1579, 1453, 1417, 1305, 1292, 1202, 1159, 1040, 938, 949, 841, 680 cm⁻¹. 1 H NMR (500 MHz, CD₂Cl₂) δ 8.58 (s, 1H), 8.26 (s, 1H), 7.79 (d, J = 7.3 Hz, 1H), 7.12–7.03 (m, 1H), 6.88 (s, 4H), 6.68 (d, *J* = 14.5 Hz, 8H), 3.80 (s, 24H). ¹¹B NMR (128 MHz, CD_2Cl_2) δ 2.97 (q, J_{F-B} = 52.4 Hz). ¹³C{H} NMR (126 MHz, CD_2Cl_2) [missing 1 resonance] δ 162.2 (d, J_{P-C} = 19.6 Hz), 152.9, 146.5, 140.2, 123.0, 119.4 (d, $J_{P-C} = 90.4 \text{ Hz}$), 113.3 (d, $J_{P-C} = 11.7$ Hz), 106.4, 56.6. ¹⁹F{H} NMR (376 MHz, CD₂Cl₂) δ –143.74 (dd, J_{B-F} = 99.8, 46.5 Hz), –153.44. ³¹P{H} NMR (203 MHz, CD₂Cl₂) δ 26.66. HRMS-ESI calcd for $C_{32}H_{36}O_8P^+$ (M – 1F⁻)⁺ 579.2143 found 579.2138 and calcd for $C_5H_4BF_3N^-$ (M - P(3,5-(MeO)₂C₆H₃)₄+)⁻ 146.0394, found 146.0396.

Tetraphenylphosphonium Trifluoro(pyridin-4-yl)borate (2F-PPh₄+). Synthesized via the same procedure as 1c Tetraphenylphosphonium chloride (328 mg, 0.875 mmol, 1.00 equiv) and potassium trifluoro(pyridin-4-yl)borate (170 mg, 0.919 mmol, 1.05 equiv) afforded 395 mg (0.813 mmol, 93%) of the product as a white solid (m.p. = 156-158 °C) using the same procedure as for 1F⁻PPh₄⁺. IR-ATR 3430, 3053, 2971, 1738, 1586, 1483, 1438, 1403, 1200, 1192, 1105, 982, 961, 813, 758, 721, 689 cm⁻¹. ¹H NMR (500 MHz, CDCl₃) δ 8.26 (d, J = 5.5 Hz, 2H), 7.93–7.83 (m, 4H), 7.74 (td, J = 7.9, 3.6 Hz, 8H), 7.63-7.54 (m, 8H), 7.44 (d, J = 5.2 Hz,2H). ¹¹B NMR (128 MHz, CDCl₃) δ 2.85 (d, $J_{\text{F-B}}$ = 52.3 Hz). 13 C{H} NMR (126 MHz, CDCl₃) [missing 1 resonance] δ 147.7, 135.8 (d, J_{P-C} = 3.1 Hz), 134.4 (d, J_{P-C} = 10.4 Hz), 130.8 (d, J_{P-C} = 12.8 Hz), 127.5, 117.5 (d, J_{P-C} = 89.5 Hz). ¹⁹F{H} NMR (376 MHz, CDCl₃) δ -145.80 (d, J_{B-F} = 78.7 Hz). ³¹P{H} NMR (203 MHz, CDCl₃) δ 23.14. HRMS-ESI calcd for $C_{24}H_{20}P^+$ (M – 2F⁻)⁺ 339.1298 found 339.1302 and calcd for $C_5H_4BF_3N^-\ (M-PPh_4^+)^-$ 146.0394, found 146.0399.

Potassium Tris(4-(t-butyl)phenyl)(pyridin-3-yl)borate (1t-Bu-K+). In a two-necked round-bottomed flask equipped with a septum and addition funnel, freshly burnished magnesium turnings (224 mg, 9.21 mmol, 5.11 equiv) were suspended in THF (10 mL) and 4 drops of dibromoethane were added as an initiator under an argon atmosphere. Upon heating the flask to 40 °C, a solution of 10 mL of THF and 1.918 g (9.00 mmol, 5.00 equiv) 1-bromo-4-t-butyl-benzene was added dropwise over the course of 30 min and the reaction mixture was stirred for an additional 4 h (during which the magnesium was fully consumed). After cooling the resulting solution to 0 °C, 333 mg (1.80 mmol, 1.00 equiv) of potassium trifluoro-

(pyridin-3-yl)borate was added in one portion and the reaction mixture was stirred for 1 h at room temperature and then 14 h at reflux. Concentrated aqueous K2CO3 (10 mL) was used to quench the reaction, and the product was extracted twice with 50 mL portions of DCM. The combined organic material was concentrated with a rotary evaporator, and the resulting salt was dissolved in a minimal amount of DCM (~3 mL) and triturated into 100 mL of hexanes to afford 744 mg (1.41 mmol, 78%) of the product as a white solid (m.p. >220 °C). Note: this compound could consist of a mixture of magnesium and potassium cations, and yields and molar amounts for subsequent reactions were calculated based upon the latter ion. IR-ATR 3233, 3167, 3115, 3062, 3005, 2962, 2866, 1608, 1528, 1496, 1390, 1286, 807 cm $^{-1}$. ¹H NMR (500 MHz, acetone- d_6) δ 8.49 (s, 1H), 8.32 (d, J = 4.8 Hz, 1H), 8.20 (d, J = 7.7 Hz, 1H), 7.45 (dd, J =7.7, 5.3 Hz, 1H), 7.21 (d, J = 7.6 Hz, 6H), 7.07 (d, J = 8.2 Hz, 6H), 1.26 (s, 27H). ¹¹B NMR (161 MHz, acetone- d_6) δ -7.82. ¹³C{H} NMR (126 MHz, acetone- d_6) [missing 1 resonance] δ 158.3 (q, J_{B-C} = 48.1 Hz), 150.6, 150.4, 144.9, 138.2, 136.2, 123.9, 123.5, 34.5, 32.0. HRMS-ESI calcd for C₃₅H₄₃BN⁻ (M - PPh₄⁺)⁻ 488.3494, found

Tetraphenylphosphonium Tris(4-(t-butyl)phenyl)(pyridin-3-yl)borate (1t-Bu-PPh₄+). In a 25 mL round-bottomed flask, 72.6 mg (0.137 mmol, 1.00 equiv) of potassium tris(4-(t-butyl)phenyl)-(pyridin-3-yl)borate was suspended in 5 mL of DCM and a slight excess of tetraphenylphosphonium bromide (60.6 mg, 0.144 mmol, 1.05 equiv) was added along with 5 mL of a dilute solution of aqueous K₂CO₃. The resulting mixture was vigorously stirred (1400 rpm) for 1 h; at which point, 5 mL of DCM was added, and the organic layer was separated, dried with K₂CO₃, and concentrated to afford 109 mg (0.132 mmol, 96%) of the product as a voluminous white powder (m.p. = 122-124 °C). Vapor diffusion using benzene and pentane was used to grow suitable crystals for X-ray crystallography. IR-ATR 3057, 2958, 2898, 2862, 1494, 1484, 1436, 1388, 1107, 807, 721, 688 cm⁻¹. ¹H NMR (500 MHz, CD₂Cl₂) δ 8.46 (s, 1H), 8.00 (dd, J = 4.8, 1.9 Hz, 1H), 7.92-7.83 (m, 4H), 7.69 (td, J = 7.8, 3.5 Hz, 8H), 7.65(br. s, 1H), 7.58 (ddd, J = 13.1, 8.4, 1.3 Hz, 8H), 7.26 (dt, J = 5.6, 2.9 Hz, 6H), 7.06 (d, J = 8.0 Hz, 7H), 6.87 (dd, J = 7.5, 4.7 Hz, 1 Hz), 1.25 (s, 27H). ¹¹B NMR (161 MHz, CD_2Cl_2) δ –7.86. ¹³C{H} NMR (126 MHz, $\mathrm{CD_2Cl_2}$) δ 159.7 (q, $J_{\mathrm{B-C}}$ = 48.9 Hz), 155.4, 145.1, 144.6, 141.6, 136.3 (d, J_{P-C} = 3.2 Hz), 135.6, 134.9 (d, J_{P-C} = 10.2 Hz), 131.2 (d, $J_{P-C} = 13.0 \text{ Hz}$), 124.1, 123.3, 122.5, 118.0 (d, $J_{P-C} = 89.5 \text{ Hz}$), 34.4, 32.0. 31 P{H}NMR (203 MHz, CD₂Cl₂) δ 23.27. HRMS-ESI calcd for $C_{24}H_{20}P^+$ (M - 1t-Bu⁻)⁺ 339.1298, found 339.1297 and calcd for $C_{35}H_{43}BN^-$ (M - PPh_4^+)⁻ 488.3494, found 488.3493.

Tetrakis[4-(dimethylamino)phenyl]phosphonium Tris(4-(tbutyl)phenyl)(pyridin-3-yl)borate (1t- $\dot{B}u^-$ P(4- $Me_2NC_6H_4)_4^+$). Potassium tris(4-(t-butyl)phenyl)(pyridin-3-yl)borate (72.7 mg, 0.138 mmol, 1.00 equiv) and a slight excess of tetrakis(4-(dimethylamino)phenyl)phosphonium chloride (79.2 mg, 0.145 mmol, 1.05 equiv) afforded 135 mg (0.135 mmol, 98%) of the product as an off-white voluminous solid (m.p. = 145-148 °C) using the same procedure as for the tetraphenylphosphonium salt. IR-ATR 3056, 2952, 2862, 1592, 1517, 1370, 1206, 1104, 808, 774 cm⁻¹. ¹H NMR (500 MHz, CD_2Cl_2) δ 8.51 (s, 1H), 8.04 (dd, I = 4.9, 1.9 Hz, 1H), 7.84 (d, I =7.3 Hz, 1H), 7.36-7.19 (m, 14H), 7.09 (d, J = 8.2 Hz, 6H), 7.01 (dd, J = 7.5, 4.9 Hz, 1H), 6.77 (dd, J = 9.1, 2.6 Hz, 8H), 3.05 (s, 24H), 1.27 (s, 27). ¹¹B NMR (161 MHz, CD_2Cl_2) δ -7.86. ¹³C{H} NMR (126 MHz, CD_2Cl_2) [missing 1 resonance] δ 159.9 (q, J_{B-C} = 53.1 Hz), 155.9, 154.1, 144.7, 144.6, 142.0, 135.7 (d, $J_{P-C} = 5.8$ Hz), 135.5, 124.0, 122.4, 112.5 (d, $J_{P-C} = 13.3 \text{ Hz}$), 104.3 (d, $J_{P-C} = 103.3 \text{ Hz}$), 40.3, 34.4, 32.0. ³¹P{H} NMR (203 MHz, CD₂Cl₂) δ 18.74. HRMS-ESI calcd for $C_{32}H_{40}N_4P^+$ (M – 1*t*-Bu⁻)⁺ 511.2986, found 511.2982 and calcd for $C_{35}H_{43}BN^-$ (M - P(4-Me₂NC₆H₄)₄+)⁻ 488.3494, found 488.3496.

Tetrakis(3,5-dimethoxyphenyl)phosphonium Tris(4-(t-butyl)phenyl)(pyridin-3-yl)borate (1t-Bu⁻ P(3,5-(MeO)₂C₆H₃)₄⁺). Potassium tris(4-(t-butyl)phenyl)(pyridin-3-yl)borate (67.6 mg, 0.128 mmol, 1.00 equiv) and a slight excess of tetrakis(3,5-dimethoxyphenyl)phosphonium chloride (82.7 mg, 0.135 mmol, 1.05 equiv) afforded 132 mg (0.123 mmol, 96%) of the product as an

off-white voluminous solid (m.p. = 95–98 °C) using the same procedure as the tetraphenylphosphonium salt. IR-ATR 3057, 3006, 2959, 2899, 2864, 2838, 1581, 1453, 1416, 1307, 1292, 1205, 1161, 1061, 1041, 808, 679 cm⁻¹. ¹H NMR (500 MHz, CD₂Cl₂) δ 8.50 (s, 1H), 8.04 (s, 1H), 7.87 (s, 1H), 7.27 (s, 6H), 7.17–6.99 (m, 7H), 6.86 (s, 4H), 6.68 (d, J = 14.5 Hz, 8H), 3.79 (s, 24H), 1.28 (s, 27H). ¹¹B NMR (161 MHz, CD₂Cl₂) δ –7.86. ¹³C{H} NMR (126 MHz, CD₂Cl₂) [missing one resonance] δ 162.8 (d, J_{P-C} = 19.6 Hz), 157.5, 144.4, 143.3, 136.0, 135.7, 126.5, 123.2, 122.1, 119.4 (d, J_{P-C} = 90.3 Hz), 113.3 (d, J_{P-C} = 11.6 Hz), 106.3 (d, J_{P-C} = 2.6 Hz), 56.6, 34.4, 31.9. ³¹P{H} NMR (203 MHz, CD₂Cl₂) δ 26.67. HRMS-ESI calcd for C₃₂H₃₆O₈P⁺ (M – 1*t*-Bu⁻)+ 579.2143, found 579.2145 and calcd for C₃₅H₄₃BN⁻ (M – P(3,5-(MeO)₂C₆H₃)₄+)⁻ 488.3494, found 488.3481.

Potassium Tris(4-(t-butyl)phenyl)(pyridin-4-yl)borate (2t-Bu- K^{+}). This compound was synthesized via the same procedure as for the 3-pyridyl derivative but with a modified purification method. Magnesium (224 mg, 9.21 mmol, 5.12 equiv), 1-bromo-4-t-butylbenzene (1.92 g, 9.00 mmol, 5.00 equiv), and trifluoro(pyridin-4yl)borate (333 mg, 1.80 mmol, 1.00 equiv) afforded the crude product as a yellow oil, which was dissolved in acetone and triturated into hexane at 0 °C. After decanting the liquid away from the yellow oil at the bottom of the flask, it was taken up in DCM, concentrated, and dried under vacuum to afford 332 mg (0.629 mmol, 35%) of the product as a light brown solid (m.p. >220 °C). This compound appears to be unstable in solution, complicating efforts to acquire satisfactory spectra. HRMS and a fairly clean ¹H spectrum were obtained, but complete characterization was carried out on the subsequent phosphonium salts. Signals corresponding to what is likely the zwitterionic byproduct (i.e., the conjugate acid) are labeled in gray in the NMR spectrum given in the Supporting Information. Subsequent yields to the various phosphonium ions were computed as if this was a single compound. ¹H NMR (500 MHz, acetone- d_6) δ 8.26 (d, J = 5.9 Hz, 2H), 7.88 (d, J = 5.7 Hz, 2H), 7.22 (d, J = 7.7 Hz, 6H), 7.08 (d, J = 8.3 Hz, 6H), 1.26 (s, 27H). HRMS-ESI calcd for $C_{35}H_{43}BN^{-}$ (2t-Bu⁻ - K⁺)⁻ 488.3494, found 488.3506.

Tetraphenylphosphonium Tris(4-(t-butyl)phenyl)(pyridin-4-yl)borate (2t-Bu-PPh₄+). This compound was prepared using the same procedure as the 3-pyridyl tetraphenylphosphonium salt 1t-Bu⁻PPh₄⁺. Potassium tris(4-(t-butyl)phenyl)(pyridin-4-yl)borate (67.5 mg, 0.128 mmol, 1.00 equiv) and a slight excess of tetraphenylphosphonium bromide (56.3 mg, 0.134 mmol, 1.05 equiv) afforded 96 mg (0.116 mmol, 91%) of the product as an offwhite solid (m.p. = 135-140 with decomp.). Single crystals were grown for X-ray crystallography by vapor diffusion using benzene and pentane. IR-ATR 3056, 2958, 2899, 2863, 1732, 1582, 1436, 1267, 1107, 808, 795, 722, 689 cm⁻¹. ¹H NMR (500 MHz, CD₂Cl₂) δ 8.04 (d, J = 5.8 Hz, 2H), 7.89 (td, J = 7.6, 1.9 Hz, 4H), 7.70 (td, J = 8.0, 1.9 Hz, 4H)3.6 Hz, 8H), 7.58 (ddd, J = 13.0, 8.4, 1.3 Hz, 8H), 7.37 (s, 2H), 7.25 (t, J = 5.7 Hz, 6H), 7.07 (d, J = 8.3 Hz, 6H), 1.26 (s, 27H). ¹¹B NMR (161 MHz, CD₂Cl₂) δ -7.30. ¹³C{H} NMR (126 MHz, CD₂Cl₂) δ 159.8 (q, $J_{B-C} = 50.3 \text{ Hz}$), 146.8, 144.6, 136.3 (d, $J_{P-C} = 3.2 \text{ Hz}$), 135.7, 134.9 (d, J = 10.2 Hz), 132.0, 131.2 (d, $J_{P-C} = 12.9 \text{ Hz}$), 124.2, 123.3 (d, J_{P-C} = 4.2 Hz), 118.0 (d, J_{P-C} = 89.5 Hz), 34.4, 32.0. ³¹P{H} NMR (203 MHz, CD₂Cl₂) δ 23.29. HRMS-ESI calcd for C₂₄H₂₀P⁺ $(M - 2t-Bu^{-})^{+}$ 339.1298, found 339.1295 and calcd for $C_{35}H_{43}BN^{-}$ $(M - PPh_4^+)^-$ 488.3494, found 488.3496.

Tetrakis[4-(dimethylamino)phenyl]phosphonium Tris(4-(t-butyl)phenyl)(pyridin-4-yl)borate (2t-Bu⁻ P(4-Me₂NC₆H₄)₄+). Potassium tris(4-(t-butyl)phenyl) (pyridin-4-yl)borate (73.8 mg, 0.140 mmol, 1.00 equiv) and a slight excess of tetrakis(4-(dimethylamino)phenyl)phosphonium bromide (80.4 mg, 0.147 mmol, 1.05 equiv) afforded 132 mg (0.132 mmol, 94%) of the product as a pale yellow solid (m.p = 154–157 °C) using the same procedure as for 2t-Bu⁻PPh₄+. IR-ATR 3055, 2950, 2862, 1592, 1517, 1370, 1206, 1104, 809, 774 cm⁻¹. ¹H NMR (500 MHz, CD₂Cl₂) δ 8.08 (d, J = 5.6 Hz, 2H), 7.36 (s, 2H), 7.33–7.23 (m, 14H), 7.08 (d, J = 8.2 Hz, 6H), 6.76 (dd, J = 9.2, 2.6 Hz, 8H), 3.05 (s, 24H), 1.26 (s, 27H). ¹¹B NMR (161 MHz, CD₂Cl₂) δ –7.27. ¹³C{H} NMR (126 MHz, CD₂Cl₂) δ 159.6 (q, J_{C-B} = 51.7 Hz), 154.1 (d, J_{P-C} = 2.5 Hz), 146.6, 144.6,

135.7, 135.6 (d, J_{P-C} = 11.7 Hz), 135.0, 132.9, 132.0, 124.3, 123.3, 112.5 (d, J_{P-C} = 13.4 Hz), 104.2 (d, J_{P-C} = 103.4 Hz), 40.3, 34.4, 32.0. ³¹P{H} NMR (203 MHz, CD₂Cl₂) δ 18.74. HRMS-ESI calcd for $C_{32}H_{40}N_4P^+$ (M – 2t-Bu⁻)⁺ 511.2986, found 511.2982 and calcd for $C_{35}H_{43}BN^-$ (M – P(4-Me₂NC₆H₄)₄+)⁻ 488.3494, found 488.3496.

Potassium Tris(3,5-dimethoxyphenyl)(pyridin-4-yl)borate (*2OMe2*[−] K⁺). Magnesium (258 mg, 10.6 mmol, 5.10 equiv), 1-bromo-3,5-dimethoxybenzene (2.25 g, 10.4 mmol, 5.00 equiv), and trifluoro(pyridin-4-yl)borate (383 mg, 2.08 mmol, 1.00 equiv) were used to synthesize the title compound following the same procedure as for 1t-Bu[−]K⁺. The resulting oil was dissolved in minimal ethyl acetate, and small white crystals formed. They were collected via filtration and washed with cold ethyl acetate to afford 408 mg (0.756 mmol, 36%) of the product as a white solid (m.p. = 178−180). IR-ATR 3104, 3052, 2932, 2893, 2835, 1573, 1455, 1404, 1273, 1197, 1147, 1063, 1046, 837 cm^{−1}. ¹H NMR (500 MHz, acetone- d_6) δ 8.40 (d, J = 6.5 Hz, 2H), 8.04 (d, J = 6.0 Hz, 2H), 6.52 (s, 6H), 6.11 (t, J = 2.4 Hz, 3H), 3.61 (s, 18H). ¹¹B NMR (161 MHz, acetone- d_6) δ −5.70. ¹³C{H} NMR (126 MHz, acetone- d_6) δ 162.6 (q, J_{B-C} = 51.3 Hz), 160.3, 136.4, 134.1, 114.4, 106.9, 95.8, 54.9. HRMS-ESI calcd for C₂₉H₃₁BNO₆[−] (M − K⁺)[−] 500.2249, found 500.2236.

Tetraphenylphosphonium Tris(3,5-dimethoxyphenyl)(pyridin-4yl)borate (20Me2⁻ PPh₄⁺). This species was prepared following the procedure for 1t-Bu-K+, and 73.9 mg (0.137 mmol, 1.00 equiv) of potassium tris(3,5-dimethoxyphenyl)(pyridin-4-yl)borate and 60.3 mg (0.143 mmol, 1.05 equiv) of tetraphenylphosphonium bromide afforded 81.0 mg (0.0965 mmol, 70%) of the title compound as an off-white solid (m.p. 75-80 °C w/ decomp.). IR-ATR 3049, 2991, 2937, 2828, 1575, 1436, 1403, 1269, 1143, 1108, 1061, 996, 839, 722, 688 cm⁻¹. ¹H NMR (500 MHz, CD₂Cl₂) δ 8.05 (d, J = 5.0 Hz, 2H), 7.86 (t, J = 7.4 Hz, 4H), 7.68 (td, J = 7.9, 3.6 Hz, 8H), 7.59 (dd, J = 7.8) 13.1, 7.8 Hz, 8H), 7.33 (s, 2H), 6.57 (s, 6H), 6.04 (s, 3H), 3.61 (s, 18H). ¹¹B NMR (161 MHz, CD₂Cl₂) δ -6.35. ¹³C{H} NMR (126 MHz, CD_2Cl_2) δ 165.6 (q, J_{B-C} = 49.8 Hz), 159.5 (d, J_{P-C} = 4.1 Hz), 146.8, 136.3 (d, J_{P-C} = 3.3 Hz), 134.9 (d, J_{P-C} = 10.1 Hz), 132.1, 131.2 (d, J_{P-C} = 12.9 Hz), 118.1 (d, J_{P-C} = 89.5 Hz), 113.9, 110.6, 106.6, 95.5, 55.3. 31 P{H} NMR (203 MHz, CD₂Cl₂) δ 23.21. HRMS-ESI calcd for C₂₄H₂₀P⁺ (M – **20Me2**⁻)⁺ 339.1298, found 399.1290 and calcd for C₂₉H₃₁BNO₆⁻ (M – PPh₄⁺)⁻ 500.2249, found 500.2244.

Tetrakis[4-(dimethylamino)phenyl]phosphonium Tris(3,5dimethoxyphenyl)(pyridin-4-yl)-borate (20Me2- P(4- $Me_2NC_6H_4J_4^+$). This species was prepared following the procedure for 1t-Bu-K+, and 78.4 mg (0.145 mmol, 1.00 equiv) of potassium phosphonium tris(3,5-dimethoxyphenyl)(pyridin-4-yl)borate and 83.5 mg (0.152 mmol, 1.05 equiv) of tetrakis [4-(dimethyl-amino)phenyl]phosphonium chloride afforded 106.8 mg (0.105 mmol, 73%) of the title compound as an off-white sticky solid (m.p. 90-93 °C). IR-ATR 3044, 2987, 2933, 2826, 1592, 1518, 1444, 1371, 1269, 1198, 1144, 1104, 1062, 813 cm $^{-1}.$ ^{1}H NMR (500 MHz, $\text{CD}_{2}\text{Cl}_{2})$ δ 8.11 (d, J = 5.0 Hz, 2H, 7.36 - 7.24 (m, 10H), 6.78 (dd, J = 9.1, 2.7 Hz, 8H),6.61-6.53 (m, 6H), 6.06 (t, J = 2.5 Hz, 3H), 3.63 (s, 18H), 3.05 (s, 24H). ¹¹B NMR (161 MHz, CD₂Cl₂) δ –6.33. ¹³C{H} NMR (126 MHz, CD_2Cl_2) δ 165.7 (q, J_{B-C} = 49.1 Hz), 159.5 (q, J_{B-C} = 3.9 Hz), 154.1, 147.0, 135.5 (d, J_{P-C} = 11.6 Hz), 132.0, 113.8, 112.5 (d, J_{P-C} = 13.4 Hz), 110.5, 104.2 (d, J_{P-C} = 103.3 Hz), 95.6, 55.3, 40.3. ${}^{31}P\{H\}$ NMR (203 MHz, CD_2Cl_2) δ 18.73. HRMS-ESI calcd for $C_{32}H_{40}N_4P^+$ (M - 20Me2⁻)⁺ 511.2986, found 511.2988 and calcd for $C_{29}H_{31}BNO_6^-$ (M - P(4-Me₂NC₆H₄)₄+)⁻ 500.2249 found 500.2240.

Potassium Tris(4-methoxyphenyl)(pyridin-4-yl)borate (**20Me**[−]*K*⁺). This compound was prepared following the procedure for **20Me2**[−]*K*⁺, and 224 mg (9.21 mmol, 5.12 equiv) of Mg, 1.68 g (9.00 mmol, 5.00 equiv) of 1-bromo-4-methoxybenzene, and 333 mg (1.80 mmol), 1.00 equiv) were used. The resulting salt was dissolved in a minimal amount of ethyl acetate, and 271 mg (0.603 mmol, 34%) of a white solid formed (m.p. >220). IR-ATR 3124, 3072, 3004, 2949, 2833, 1734, 1617, 1589, 1566, 1495, 1263, 1223, 1178, 1032, 805, 793, 767 cm^{−1}. ¹H NMR (500 MHz, Aacetone-*d*₆) δ 8.36 (d, *J* = 6.7 Hz, 2H), 7.95 (d, *J* = 5.8 Hz, 2H), 7.11 (d, *J* = 7.9 Hz, 6H), 6.65 (d, *J* = 8.5 Hz, 6H), 3.69 (s, 9H). ¹¹B NMR (161 MHz, acetone-*d*₆) δ −6.76. ¹³C{H} NMR (126 MHz, acetone-*d*₆) [missing 2 resonances]

 δ 157.1, 137.0, 136.2, 134.0, 112.7, 54.9. HRMS-ESI calcd for $C_{26}H_{25}BNO_3^-$ (M - K $^+)^-$ 410.1932 found 410.1938.

Tetraphenylphosphonium Tris(4-methoxyphenyl)(pyridin-4-yl)borate (20Me PPh₄+). Potassium tris(4-methoxyphenyl)(pyridin-4-yl)borate (79.0 mg, 0.164 mmol, 1.00 equiv) and tetraphenylphosphonium bromide (69.0 mg, 0.164 mmol, 1.00 equiv) afforded 117 mg (0.156 mmol, 95%) of the product as a white solid (m.p. 180-182 °C) using the same procedure as for 1t-Bu⁻PPh₄⁺. IR-ATR 3047, 3012, 2953, 2897, 2828, 1585, 1494, 1436, 1267, 1233, 1106, 1033, 801, 721, 688 cm⁻¹. ¹H NMR (500 MHz, CD₂Cl₂) δ 8.05 (s, 2H), 7.88 (t, J = 7.5 Hz, 4H), 7.70 (d, J = 9.7 Hz, 8H), 7.65–7.55 (m, 8H), 7.42 (s, 2H), 7.13 (d, J = 8.0 Hz, 6H), 6.63 (d, J = 7.8 Hz, 6H), 3.70(s, 9H). ^{11}B NMR (161 MHz, CD $_2\text{Cl}_2)$ δ –7.51. $^{13}\text{C}\{\text{H}\}$ NMR (126 MHz, CD_2Cl_2) [missing one resonance] δ 156.4, 152.9 (q, J_{B-C} = 51.0 Hz), 140.7, 136.7, 136.3 (d, $J_{P-C} = 3.1 \text{ Hz}$), 134.9 (d, $J_{P-C} = 10.4 \text{ Hz}$), 132.9, 131.2 (d, J_{P-C} = 12.8 Hz), 118.0 (d, J_{P-C} = 89.5 Hz), 112.2, 55.3. 31 P{H} NMR (203 MHz, CD₂Cl₂) δ 23.25. HRMS-ESI calcd for $C_{24}H_{20}P^+$ (M – 20Me⁻)⁺ 339.1298, found 339.1304 and calcd for $C_{26}H_{25}BNO_3^-$ (M - PPh₄⁺) 410.1932, found 410.1949.

Tetraphenylphosphonium ((4-Methoxyphenyl)sulfonyl)(pyridin-4-yl)amide (4⁻ PPh₄⁺). This compound was synthesized following the literature procedure described by Zipse et al. 28 using 941 mg (10.0 mmol, 1.00 equiv) of 4-aminopyridine, 2.07 g (10.0 mmol, 1.00 equiv) of 4-methoxy-benzenesulfonyl chloride, and 3.0 mL (2.18 g, 21.5 mmol, 2.15 equiv) of triethylamine to afford 2.17 g (8.21 mmol, 82%) of the neutral sulfonamide. A portion of this material (365 mg, 1.38 mmol, 1.00 equiv) along with 579 mg (1.38 mmol, 1.00 equiv) of tetraphenylphosphonium bromide gave 537 mg (0.892 mmol, 65%) of the product as a white solid also as described by Zipse et al.²⁸ Its spectra are in agreement with the literature data. ¹H NMR (500 MHz, CDCl₃) δ 7.89–7.81 (m, 8H), 7.73 (td, J = 7.9, 3.6 Hz, 8H), 7.62– 7.52 (m, 8H), 6.82-6.71 (m, 4H), 3.73 (s, 3H). ¹³C{H} NMR (126 MHz, CDCl₃) δ 160.3, 157.7, 148.7, 138.8, 135.7 (d, $J_{P-C} = 3.2 \text{ Hz}$), 134.3 (d, J_{P-C} = 10.3 Hz), 130.7 (d, J_{P-C} = 12.8 Hz), 128.5, 117.4 (d, J_{P-C} = 89.5 Hz), 116.1, 113.0 55.2. ³¹P{H} NMR (203 MHz, CDCl₃) δ 23.06.

Tetraphenylphosphonium ((4-Methoxyphenyl)sulfonyl)(pyridin-3-yl)amide (3- PPh₄+). This compound was synthesized using the same procedure as for 4⁻PPh₄⁺ using 941 mg (10.0 mmol, 1.00 equiv) of 3-aminopyridine, 2.07 g (10.0 mmol, 1.00 equiv) of 4methoxybenzenesulfonyl chloride, and 3.0 mL (2.18 g, 21.5 mmol, 2.15 equiv) of triethylamine to afford 1.99 g (7.53 mmol, 75%) of the neutral sulfonamide. A portion of this material (365 mg, 1.38 mmol, 1.00 equiv) and tetraphenyl-phosphonium bromide (579 mg, 1.38 mmol) gave 496 mg (0.822 mmol, 65%) of the product as a white solid (m.p. 160-161 °C). IR-ATR 3054, 3022, 2938, 2837, 1594, 1571, 1473, 1436, 1399, 1286, 1232, 1122, 1108, 1082, 968, 802, 721, 688 cm⁻¹. ¹H NMR (500 MHz, acetone- d_6) δ 8.10 (d, J = 2.7 Hz, 1H), 8.04-7.96 (m, 4H), 7.89-7.82 (m, 16H), 7.78-7.72 (m, 2H), 7.55 (dd, J = 4.6, 1.5 Hz, 1H), 7.24 (ddd, J = 8.4, 2.7, 1.5 Hz, 2H), 6.80-6.76 (m, 1H), 6.73 (dd, J = 8.3, 4.5 Hz, 1H), 3.74 (s, 3H). $^{13}\text{C}\{\text{H}\}$ NMR (126 MHz, acetone- d_6) δ 160.1, 148.0, 144.2, 140.7, 136.0, 135.5 (d, J_{P-C} = 3.2 Hz), 134.8 (d, J_{P-C} = 10.3 Hz), 130.6 (d, $J_{P-C} = 12.9 \text{ Hz}$), 128.3, 125.07, 122.4, 118.1 (d, $J_{P-C} = 89.5 \text{ Hz}$), 112.6, 54.7. $^{31}P\{H\}$ NMR (203 MHz, acetone- d_6) δ 22.99. HRMS-ESI calcd for $C_{24}H_{20}P^+$ (M - 3⁻)⁺ 339.1298, found 339.1303 and calcd for $C_{12}H_{11}N_2O_3S^-$ (M - PPh₄⁺)⁻ 263.0495 found 263.0501.

Tetraphenylphosphonium ((4-Methoxyphenyl)sulfonyl)(phenyl)-amide (4-MeOC₆H₄SO₂N⁻Ph Ph_4P^+). The same procedure was used as for 4, but a different purification method was employed. Aniline (462 mg, 4.96 mmol, 1.00 equiv), 4-methoxybenzenesulfonyl chloride (1.025 g, 4.96 mmol, 1.00 equiv), and triethylamine (3.0 mL, 2.18 g, 21.5 mmol, 2.15 equiv) gave the crude product, which was recrystallized from water and acetone to give 1.19 g (4.51 mmol, 91%) of the sulfonamide. A portion of this material (90.1 mg, 0.342 mmol, 1.00 equiv) was suspended in water and deprotonated with aqueous NaOH, and then 143 mg (0.342 mmol, 1.00 equiv) of tetraphenylphosphonium bromide was added to give 202 mg (0.355 mmol, 98%) of product as a hygroscopic off-white solid (m.p. 51–56 °C). IR-ATR 3056, 1586, 1482, 1436, 1288, 1246, 1121, 1106, 1086,

995, 968, 755, 720, 688 cm $^{-1}$. $^{1}\mathrm{H}$ NMR (400 MHz, CDCl $_{3}$) δ 7.91–7.82 (m, 6H), 7.75 (td, J=7.8, 3.5 Hz, 8H), 7.64–7.51 (m, 8H), 6.97 (d, J=7.3 Hz, 2H), 6.84 (t, J=7.8 Hz, 2H), 6.72 (d, J=8.8 Hz, 2H), 6.40 (t, J=7.2 Hz, 1H), 3.73 (s, 3H). $^{13}\mathrm{C}\{\mathrm{H}\}$ NMR (101 MHz, CDCl $_{3}$) δ 159.8, 150.8, 140.1, 135.7 (d, $J_{\mathrm{P-C}}=3.1$ Hz), 134.4 (d, $J_{\mathrm{P-C}}=10.3$ Hz), 130.8 (d, $J_{\mathrm{P-C}}=12.9$ Hz), 128.6, 127.9, 121.3, 117.4 (d, $J_{\mathrm{P-C}}=89.5$ Hz), 116.0, 112.9, 55.2. $^{31}\mathrm{P}\{\mathrm{H}\}$ NMR (162 MHz, CDCl $_{3}$) δ 22.98. HRMS-ESI calcd for C $_{24}\mathrm{H}_{20}\mathrm{P}^{+}$ (M -4-MeOC $_{6}\mathrm{H}_{4}\mathrm{SO}_{2}\mathrm{N}^{-}\mathrm{Ph}$) $^{+}$ 339.1298, found 339.1303 and calcd for C $_{13}\mathrm{H}_{12}\mathrm{NO}_{3}\mathrm{S}^{-}$ (M $-\mathrm{Ph}_{4}\mathrm{P}^{+}$) $^{-}$ 262.0543 found 262.0542.

S_N2 Kinetics. Nucleophiles were weighed out in a glovebox directly into vials, and a 200 mM solution of 1-iodooctane in DCM was added, so the concentration of the salt was 20 mM. These solutions were then transferred to threaded cuvettes equipped with Mininert caps, sealed with Parafilm to limit solvent loss, and placed into the UV spectrometer, which was set at 25 °C. Spectra were collected from 300 to 600 nm every 5-20 min depending on the reaction rate. Nonlinear fits of the data were carried out at a single wavelength so that the maximum absorption did not exceed 4.0, the linearity limit for the detector. To validate this method, a single determination for each reaction except for the one with DMAP was monitored by ¹H NMR. These measurements were also carried out in CH₂Cl₂, so aromatic resonances far from the solvent signal were used to minimize integration errors. In each case, the UV-vis and NMR rate constants are in good accord and the overall result is the average of all three determinations except for 1F⁻PPh₄⁺. In this instance, an additional NMR measurement was carried out and the UV-vis data were excluded. We previously have seen non-Beer's law behavior from similar salts,³¹ and this may be the same case for this species.

Urethane Kinetics. Catalysts were weighed into a vial equipped with a tightly sealing PTFE-lined cap in a glovebox, and stock solutions of 4-methylphenyl isocyanate and butanol in CDCl3 were added via a syringe on the benchtop to achieve the desired concentrations. After thoroughly mixing the contents of each vial, they were individually transferred to NMR tubes where they were maintained at 300 K in a 400 or 500 MHz NMR magnet as well as an aluminum heating block for the slower transformations; in these latter cases, the NMR tubes were also sealed with electrical tape to prevent solvent loss. Conversions were calculated using the signal for the hydroxymethylene hydrogens in butanol and the corresponding resonance in the urethane product, or the methyl absorption in 4methylphenyl isocyanate and the urethane when butanol was the limiting reagent. Linear fits of the data to a standard second-order kinetic model were carried out, and the reported rate constants are the average of two determinations.

 pK_a Determinations. Titrations were carried out by weighing out 10 mg of a base into a 2 dram vial in a glovebox and adding 1 mL of a 20 mM CH₂Cl₂ or CHCl₃ solution of a selected indicator. The contents were shaken to dissolve the base; at which point, the presence or absence of a color change was noted.

IR Measurements. Bases were dissolved in a solution of 0.5% or 1% v/v dry cyclohexanol in CCl₄. In some cases, the base was not fully soluble, so the exact concentration is unknown. For the weakly basic pyridines, a fairly concentrated solution was required to observe the hydrogen-bonded absorption band, but in these cases, Δcm^{-1} was found to be insensitive to the exact concentration. Alternatively, a 100 mM solution of the base in CDCl₃ was prepared and explored. In both cases (CCl₄ and CDCl₃ experiments), spectra were obtained with a 0.77 mm path length IR solution cell with NaCl windows.

Computations. All M06-2X⁶¹⁻⁶³ density functional theory calculations were performed with Gaussian 16⁶⁵ at the Minnesota Supercomputer Institute for Advanced Computational Research. Geometry optimizations were initially performed with the small but efficient 3-21G basis, ⁶⁵ and then the structures were reoptimized with either the cc-pVDZ or aug-cc-pVDZ basis set. ⁶⁶ Vibrational frequencies were then computed to verify that each species is an energy minimum (no negative eigenvalues) and unscaled values were used to obtain zero-point energies, thermal corrections to the enthalpy, and entropies; small frequencies that contribute more than 0.5RT to the enthalpy correction were replaced by 0.5RT. Single-

point energies with the aug-cc-pVDZ basis set were computed for the cc-pVDZ structures (i.e., M06-2X/aug-cc-pVDZ//M06-2X/cc-pVDZ) and used in subsequent energy comparisons and calculations. For conformationally flexible anions 3, 4, and 2OMe2, molecular mechanics geometry searches were carried out in Maestro and the 20 lowest energy conformers were then optimized with the M06-2X functional and 3-21G basis set. The most favorable structure was then reoptimized with the aug-cc-pVDZ basis set. Optimized structures for the conjugate acids were determined by protonating the lowest energy base structures and optimizing them with the cc-pVDZ basis set. Subsequently, M06-2X/aug-cc-pVDZ single-point energies were computed. APT charges were obtained from the vibrational frequency calculations, and the molecular orbitals were visualized using Gaussview using cubes generated from the M06-2X/aug-cc-pVDZ calculations.

ASSOCIATED CONTENT

Data Availability Statement

The data underlying this study are available in the published article and its Supporting Information.

Supporting Information

The Supporting Information is available free of charge at https://pubs.acs.org/doi/10.1021/acs.joc.3c00523.

Kinetic data, IR and NMR spectra, computed structures and energies, single-crystal X-ray structure determinations, and the complete citation to ref 64 (PDF)

Accession Codes

CCDC 2247331–2247332 contain the supplementary crystallographic data for this paper. These data can be obtained free of charge via www.ccdc.cam.ac.uk/data_request/cif, or by emailing data_request/cif, or by contacting The Cambridge Crystallographic Data Centre, 12 Union Road, Cambridge CB2 1EZ, UK; fax: +44 1223 336033.

AUTHOR INFORMATION

Corresponding Author

Steven R. Kass — Department of Chemistry, University of Minnesota, Minneapolis, Minnesota \$5455, United States; orcid.org/0000-0001-7007-9322; Email: kass@umn.edu

Authors

Stephen H. Dempsey – Department of Chemistry, University of Minnesota, Minneapolis, Minnesota 55455, United States Alex Lovstedt – Department of Chemistry, University of Minnesota, Minneapolis, Minnesota 55455, United States

Complete contact information is available at: https://pubs.acs.org/10.1021/acs.joc.3c00523

Notes

The authors declare no competing financial interest.

ACKNOWLEDGMENTS

We thank Dr. Victor G. Young of the X-Ray Crystallographic Laboratory for assistance in determining the reported X-ray crystal structures. Generous support from the National Science Foundation (CHE-1955186), the donors of the American Chemical Society Petroleum Research Fund (ACS PRF 65096-ND4), and the Minnesota Supercomputing Institute for Advanced Computational Research are also gratefully acknowledged.

REFERENCES

- (1) Schreiner, P. R. Metal-Free Organocatalysis through Explicit Hydrogen Bonding Interactions. *Chem. Soc. Rev.* **2003**, *32*, 289–296.
- (2) List, B. Introduction: Organocatalysis. Chem. Rev. 2007, 107, 5413-5415.
- (3) Wittkopp, A.; Schreiner, P. R. Metal-Free, Noncovalent Catalysis of Diels-Alder Reactions by Neutral Hydrogen Bond Donors in Organic Solvents and in Water. *Chem. Eur. J.* **2003**, *9*, 407–414.
- (4) Miyabe, H.; Takemoto, Y. Discovery and Application of Asymmetric Reaction by Multi-Functional Thioureas. *Bull. Chem. Soc. Jpn.* **2008**, *81*, 785–795.
- (5) Samet, M.; Buhle, J.; Zhou, Y.; Kass, S. R. Charge-Enhanced Acidity and Catalyst Activation. *J. Am. Chem. Soc.* **2015**, *137*, 4678–4680.
- (6) Riegel, G. F.; Kass, S. R. N-Vinyl and N-Aryl Hydroxypyridinium Ions: Charge-Activated Catalysts with Electron-Withdrawing Groups. *J. Org. Chem.* **2020**, 85, 6017–6026.
- (7) Fan, Y.; Kass, S. R. Electrostatically Enhanced Thioureas. *Org. Lett.* **2016**, *18*, 188–191.
- (8) Ma, J.; Kass, S. R. Asymmetric Arylation of 2,2,2-Trifluoroacetophenones Catalyzed by Chiral Electrostatically-Enhanced Phosphoric Acids. *Org. Lett.* **2018**, *20*, 2689–2692.
- (9) Ma, J.; Kass, S. R. Electrostatically Enhanced Phosphoric Acids and Their Applications in Asymmetric Friedel–Crafts Alkylations. *J. Org. Chem.* **2019**, *84*, 11125–11134.
- (10) Ma, J.; Kass, S. R. Electrostatically Enhanced Phosphoric Acids: A Tool in Brønsted Acid Catalysis. *Org. Lett.* **2016**, *18*, 5812–5815.
- (11) Riegel, G. F.; Takashige, K.; Lovstedt, A.; Kass, S. R. Charge-Activated TADDOLs: Recyclable Organocatalysts for Asymmetric (Hetero-)Diels—Alder Reactions. *J. Phys. Org. Chem.* **2022**, *35*, e4355.
- (12) Smajlagic, I.; Durán, R.; Pilkington, M.; Dudding, T. Cyclopropenium Enhanced Thiourea Catalysis. *J. Org. Chem.* **2018**, 83, 13973–13980.
- (13) Smajlagic, I.; White, B.; Azeez, O.; Pilkington, M.; Dudding, T. Organocatalysis Linked to Charge-Enhanced Acidity with Superelectrophilic Traits. *ACS Catal.* **2022**, *12*, 1128–1138.
- (14) Anzabi, M. Y.; Yazdani, H.; Bazgir, A. Electrostatically Enhanced Sulfuric Acid: A Strong Brønsted Acidic Catalyst for Multi-Component Reactions. *Catal. Lett.* **2019**, *149*, 1934–1940.
- (15) Palomo, C.; Oiarbide, M.; López, R. Asymmetric Organocatalysis by Chiral Bronsted Bases: Implications and Applications. *Chem. Soc. Rev.* **2009**, *38*, 632–653.
- (16) Fu, X.; Tan, C.-H. Mechanistic Considerations of Guanidine-Catalyzed Reactions. *Chem. Commun.* **2011**, *47*, 8210–8222.
- (17) Henry, L. Formation Synthétique d'Alcools Nitrés. Bull. Soc. Chim. Fr. 1895, 120, 1265–1268.
- (18) Leow, D.; Tan, C. H. Chiral Guanidine Catalyzed Enantioselective Reactions. *Chem. Asian J.* **2009**, *4*, 488–507.
- (19) Boyle, P. H.; Convery, M. A.; Davis, A. P.; Hosken, G. D.; Murray, B. A. Deportonation of Nitroalkanes by Bicyclic Amidine and Guanidine Bases; Evidence for Molecular Recognition within a Catalytic Cycle for C–C Bond Formation. *J. Chem. Soc., Chem. Commun.* 1992, 239–242.
- (20) Terada, M.; Ube, H.; Yaguchi, Y. Axially Chiral Guanidine as Enantioselective Base Catalyst for 1,4-Addition Reaction of 1,3-Dicarbonyl Compounds with Conjugated Nitroalkenes. *J. Am. Chem. Soc.* **2006**, 128, 1454–1455.
- (21) Shen, J.; Nguyen, T. T.; Goh, Y. P.; Ye, W.; Fu, X.; Xu, J.; Tan, C. H. Chiral Bicyclic Guanidine-Catalyzed Enantioselective Reactions of Anthrones. *J. Am. Chem. Soc.* **2006**, *128*, 13692–13693.
- (22) Zhao, G. L.; Shi, Y. L.; Shi, M. Synthesis of Functionalized 2H-1-Benzopyrans by DBU-Catalyzed Reactions of Salicylic Aldehydes with Allenic Ketones and Esters. *Org. Lett.* **2005**, *7*, 4527–4530.
- (23) Ibrahim, M. A.; El-Gohary, N. M.; Said, S. Synthesis of Heteroannulated Chromeno[2,3-b]Pyridines: DBU Catalyzed Reactions of 2-Amino-6-Methylchromone-3-Carboxaldehyde with Some Heterocyclic Enols and Enamines. *J. Heterocycl. Chem.* **2016**, *53*, 117–120.

- (24) Yang, J.; Bao, Y.; Zhou, H.; Li, T.; Li, N.; Li, Z. Highly Efficient Synthesis of N¹-Substituted 1H-Indazoles by DBU-Catalyzed Aza-Michael Reaction of Indazole with Enones. *Synthesis* **2016**, *48*, 1139–1146.
- (25) Steglich, W.; Höfle, G. N,N-Dimethyl-4-Pyridinamine, a Very Effective Acylation Catalyst. *Angew. Chem., Int. Ed. Engl.* **1969**, 8, 981–981.
- (26) Höfle, G.; Steglich, W.; Vorbrüggen, H. 4-Dialkylaminopyridines as Highly Active Acylation Catalysts. [New Synthetic Method (25)]. Angew. Chem., Int. Ed. Engl. 1978, 17, 569–583.
- (27) Heinrich, M. R.; Klisa, H. S.; Mayr, H.; Steglich, W.; Zipse, H. Enhancing the Catalytic Activity of 4-(Dialkylamino)Pyridines by Conformational Fixation. *Angew. Chem., Int. Ed.* **2003**, 42, 4826–4828.
- (28) Helberg, J.; Ampßler, T.; Zipse, H. Pyridinyl Amide Ion Pairs as Lewis Base Organocatalysts. J. Org. Chem. 2020, 85, 5390-5402.
- (29) Petruzziello, D.; Gualandi, A.; Giaffar, H.; Lopez-Carrillo, V.; Cozzi, P. G. The Facile and Direct Formylation of Organoboron Aromatic Compounds with Benzodithiolylium Tetrafluoroborate. *Eur. J. Org. Chem.* **2013**, 2013, 4909–4917.
- (30) Lovstedt, A.; Dempsey, S. H.; Kass, S. R. Structure Determination of a Bis[4-(di-n-butylamino)phenyl](pyridin-3-yl)-borane Tetramer Highlighting a Unique Geometric Conformation of the Core 16-Membered Ring. Acta Crystallogr., Sect. C: Struct. Chem. 2023, 79, 170–176.
- (31) Dempsey, S. H.; Kass, S. R. Liberating the Anion: Evaluating Weakly Coordinating Cations. J. Org. Chem. 2022, 87, 15466–15482.
- (32) Six, C.; Richter, F. Isocyanates, Organic. *Ullmann's Encyclopedia of Industrial Chemistry*, Vol. 20, Wiley-VCH Verlag GmbH & Co.: Weinheim, 2012, pp. 63–82.
- (33) Wohlfarth, C. Pure Liquids: Data. Landolt-Bornstein. Group IV physical chemistry. *Static dielectric constants of pure liquids and binary liquid mixtures*; Madelung, O., Ed.; Springer-Verlag: New York, 1991; Vol. 6.
- (34) Burés, J. Variable Time Normalization Analysis: General Graphical Elucidation of Reaction Orders from Concentration Profiles. *Am. Ethnol.* **2016**, *55*, 16084–16087.
- (35) Matthews, W. S.; Bares, J. E.; Bartmess, J. E.; Cornforth, F. J.; Drucker, G. E.; McCallum, R. J.; McCollum, G. J.; Vanier, N. R.; Bordwell, F. G.; Margolin, Z. Equilibrium Acidities of Carbon Acids. VI. Establishment of an Absolute Scale of Acidities in Dimethyl Sulfoxide Solution. J. Am. Chem. Soc. 1975, 97, 7006–7014.
- (36) Hunter, E. P. L.; Lias, S. G. Evaluated Gas Phase Basicities and Proton Affinities of Molecules: An Update. *J. Phys. Chem. Ref. Data* **1998**, 27, 413–656.
- (37) Cioslowski, J. A New Population Analysis Based on Atomic Polar Tensors. J. Am. Chem. Soc. 1989, 111, 8333-8336.
- (38) Schafman, B. S.; Wenthold, P. G. Regioselectivity of Pyridine Deprotonation in the Gas Phase. J. Org. Chem. 2007, 72, 1645–1651.
- (39) Hansch, C.; Leo, A.; Taft, R. W. A Survey of Hammett Substituent Constants and Resonance and Field Parameters. *Chem. Rev.* 1991, 91, 165–195.
- (40) Hogen-Esch, T. E.; Smid, J. Studies of Contact and Solvent-Separated Ion Pairs of Carbanions. I. Effect of Temperature, and Solvent. *J. Am. Chem. Soc.* **1966**, *88*, 307–318.
- (41) Smid, J. The Discovery of Two Kinds of Ion Pairs. J. Polym. Sci., Part A: Polym. Chem. 2004, 42, 3655–3667.
- (42) Pliego, J. R.; Piló-Veloso, D. Effects of Ion-Pairing and Hydration on the S_NAr Reaction of the F⁻ with p-Chlorobenzonitrile in Aprotic Solvents. *Phys. Chem. Chem. Phys.* **2008**, *10*, 1118–1124.
- (43) Alunni, S.; Pero, A.; Reichenbach, G. Reactivity of Ions and Ion Pairs in the Nucleophilic Substitution Reaction on Methyl P-Nitrobenzenesulfonate. J. Chem. Soc., Perkin Trans. 2 1998, 8, 1747–1750
- (44) Pregosin, P. S. Applications of NMR Diffusion Methods with Emphasis on Ion Pairing in Inorganic Chemistry: A Mini-Review. *Mag. Res. Chem.* **2017**, *55*, 405–413.
- (45) The 3-pyridyl derivatives of the electron-rich borates **20Me**⁻ **PPh**₄⁺ and **20Me2**⁻ **PPh**₄⁺ were synthesized, but clean samples were

- not obtained by recrystallization, and therefore, they were not studied further.
- (46) The frontier molecular orbital containing the nitrogen lone pair of electrons for **2OMe2** (HOMO -2, -4.43 eV) can be incorporated into Figure 6 with a little effect on the linear correlation (i.e., ln k = 2.65 HOMO (or HOMO -1) + 6.97, $r^2 = 0.936$. This is not the case for **2OMe**, but its frontier orbitals spanning from -3.97 to -5.05 eV (HOMO to HOMO -3) have little to no electron density for the nitrogen lone pair of electrons.
- (47) Izutsu, K. Electrochemistry in Nonaqueous Solutions: Second Edition. *Electrochemistry in Nonaqueous Solutions: Second Edition* 2009, 1–415, DOI: 10.1002/9783527629152.
- (48) Richard, N. A.; Charlton, G. D.; Dyker, C. A. Enhancing Catalytic Activity of Pyridines via Para-Iminophosphorano Substituents. *Org. Biomol. Chem.* **2021**, *19*, 9167–9171.
- (49) Xu, S.; Held, I.; Kempf, B.; Mayr, H.; Steglich, W.; Zipse, H. The DMAP-Catalyzed Acetylation of Alcohols—A Mechanistic Study (DMAP= 4-(Dimethylamino)pyridine). *Chem. Eur. J.* **2005**, *11*, 4751–4757.
- (50) Chang, M.-C; Chen, S.-A. Kinetics and Mechanism of Urethane Reactions: Phenyl Isocyanate—Alcohol Systems. *J. Polym. Sci. A: Polym. Chem.* 1987, 25, 2543—2559, DOI: 10.1002/pola.1987.080250919.
- (51) Silva, A. L.; Bordado, J. C. Recent Developments in Polyurethane Catalysis: Catalytic Mechanisms Review. *Catal. Rev.* **2004**, *46*, 31–51.
- (52) Wurz, R. P. Chiral Dialkylaminopyridine Catalysts in Asymmetric Synthesis. *Chem. Rev.* **2007**, *107*, 5570–5595.
- (53) Müller, C. E.; Schreiner, P. R. Organocatalytic Enantioselective Acyl Transfer onto Racemic as well as meso Alcohols, Amines, and Thiols. *Angew. Chem., Int. Ed.* **2011**, *50*, 6012–6042.
- (54) Enríquez-García, Á.; Kündig, E. P. Desymmetrisation of meso-Diols Mediated by Non-Enzymatic Acyl Transfer Catalysts. *Chem. Soc. Rev.* **2012**, *41*, 7803–7831.
- (55) Fujii, K.; Mitsudo, K.; Mandai, H.; Korenaga, T.; Suga, S. Enantioselective Acyl Migration Reactions of Furanyl Carbonates with Chiral DMAP Derivatives. *Chem. Eur. J.* **2019**, 25, 2208–2212.
- (56) Placidi, S.; D'Intignano, T. M.; Salvio, R. Preparation of Chiral DMAP Derivatives and Investigation on their Enantioselective Catalytic Activity in Benzazetidine Synthesis and Kinetic Resolutions of Alcohols. *J. Heterocycl. Chem.* **2022**, *59*, 1626–1634.
- (57) Harris, R. K.; Becker, E. D.; Cabral De Menezes, S. M.; Goodfellow, R.; Granger, P. NMR Nomenclature. Nuclear Spin Properties and Conventions for Chemical Shifts (IUPAC Recommendations 2001). *Pure Appl. Chem.* **2001**, 1795–1818.
- (58) Li, Y.; Asadi, A.; Perrin, D. M. Hydrolytic Stability of Nitrogenous-Heteroaryltrifluoro-borates Under Aqueous Conditions At Near Neutral pH. *J. Fluorine Chem.* **2009**, *130*, 377–382.
- (59) Prakash, G. K. S.; Pertusati, F.; Olah, G. A. HF-Free, Direct Synthesis of Tetrabutylammonium Trifluoroborates. *Synthesis* **2011**, 2011, 292–302.
- (60) Batey, R. A.; Quach, T. D. Synthesis and Cross-Coupling Reactions of Tetraalkylammonium Organotrifluoroborate Salts. *Tetrahedron Lett.* **2001**, 42, 9099–9103.
- (61) Zhao, Y.; Truhlar, D. G. How Well Can New-Generation Density Functionals Describe the Energetics of Bond-Dissociation Reactions Producing Radicals? *J. Phys. Chem. A* **2008**, *112*, 1095–1099.
- (62) Zhao, Y.; Truhlar, D. G. The M06 Suite of Density Functionals for Main Group Thermochemistry, Thermochemical Kinetics, Noncovalent Interactions, Excited States, and Transition Elements: Two New Functionals and Systematic Testing of Four M06-Class Functionals and 12 Other Functionals. *Theor. Chem. Acc.* 2008, 120, 215–241.
- (63) Zhao, Y.; Truhlar, D. G. Density Functionals with Broad Applicability in Chemistry. *Acc. Chem. Res.* **2008**, *41*, 157–167.
- (64) Frisch, M. J.; Trucks, G. W.; Schlegel, H. B.; Scuseria, G. E.; Robb, M. A., et al., *Gaussian 16*; Gaussian, Inc., Wallingford CT, 2016.

- (65) Ditchfield, R.; Hehre, W. J.; Pople, J. A. Self-Consistent Molecular-Orbital Methods. IX. An Extended Gaussian-Type Basis for Molecular-Orbital Studies of Organic Molecules. *J. Chem. Phys.* **2003**, *54*, 724–728.
- (66) Dunning, T. H., Jr. Gaussian Basis Sets for Use in Correlated Molecular Calculations. I. The Atoms Boron Through Neon and Hydrogen. *J. Chem. Phys.* **1989**, *90*, 1007–1023.
- (67) Maestro (version 12.9), Schrödinger, LLC, New York NY, 2021.
- (68) GaussView, Ver. 6, Dennington, R.; Keith, T.; Millam, J. Semichem Inc., Shawnee Mission, KS, 2016.